Specialization to cell-free or cell-associated spread by BAC-cloned HCMV strains not determined by the UL128-131 and RL13 loci.

Eric P. Schultz [1,4], Jean-Marc Lanchy [1], Le Zhang Day [1,3,4], Qin Yu [1], Christopher Peterson [1,2,4], Jessica Preece [1,5], and Brent J. Ryckman[1,2,3,4,5*]

Division of Biological Sciences[1], Cellular, Molecular and Microbial Biology Program[2], Biochemistry and Biophysics Program[3], Center for Biomolecular Structure and Dynamics[4], Center for Translational Medicine[5], University of Montana, Missoula, Montana, U.S.A.

*Corresponding author: Dr. Brent J. Ryckman
Division of Biological Sciences
Interdisciplinary Science Building Rm. 215
The University of Montana
Missoula, MT 59812
Tel: 406-243-6948
Fax: 406-243-4304
Email: brent.ryckman@mso.umt.edu

ABSTRACT

A widely held view is that clinical isolates of human cytomegalovirus (HCMV) are cell-associated and that mutations affecting the UL128-131 and RL13 loci arise during subsequent passage in culture and lead to the appearance of a cell-free spread phenotype. To distinguish the factors influencing cell-associated and cell-free spread, we analyzed the spread characteristics of three HCMV BAC-clones; Merlin (ME), which expresses high levels of UL128-131 and harbors a frameshift mutation within RL13, and TB40/e (TB) and TR, which are both low in UL128-131 and intact at RL13. Quantitation of the number of newly infected cells over 12 days by flow cytometry revealed remarkably similar spread efficiencies in fibroblasts among strains. However, comparing the inhibition of spread by neutralizing antibodies and the quantities and infectivity of progeny virus indicated that TB and TR spread was predominately cell-free, whereas spread of ME was predominantly cell-associated. While transcriptional repression of UL128-131 greatly enhanced cell-free spread by ME, the efficiency of the cell-associated mode was not affected. Spread in epithelial cultures was highly cell-associated for all strains, and ME was the most efficient. Repression of UL128-131 reduced the efficiency of ME spread in epithelial cells, but did not affect the predominate mode of spread. Spread in RL13-expressing cells was comparably reduced for all strains, and more pronounced in fibroblasts than in epithelial cells. RL13 effects could not be clearly explained by changes in production, release, or infectivity of progeny virus, and there were no changes to the proclivity of strains for cell-free or cell-associated spread. In sum, the specialization of HCMV strains to cell-free spread is linked to the quantity and infectivity of cell-free progeny, which can be influenced by UL128-131 levels, but the cell-associated specialist phenotype is likely determined by factors beyond the UL128-131 or RL13 loci.

AUTHOR SUMMARY

Experimental distinctions between cell-free and cell-associated modes of spread for HCMV have been largely relativistic. When cell-free spread is inhibited by neutralizing antibodies, or if particular strain of virus is poor at cell-free spread, then the observed spread may be simply defined as “cell-associated”. However, such a view does not easily lend towards analysis of the efficiency of cell-associated spread or the factors involved. In our study, we measured the kinetics of HCMV cell-free and cell-associated spread as independent processes and show evidence that HCMV strains can be highly specialized to one or the other mode of

spread. The genetic factors that determine specialization for mode of spread are unclear, but given the genetic diversity of HCMV circulating in human populations, it seems likely that both modes of are represented. The efficacy of intervention approaches is likely affected by the mode of spread. For example, neutralizing antibodies are less effective to limit cell-associated spread. Our results provide a conceptual approach to evaluating intervention approaches such as neutralizing antibodies raised by vaccine candidates and drug compounds that target viral replication processes for their ability to limit cell-free or cell-associated modes of spread as independent processes.

36 **INTRODUCTION**

37 Intervention approaches to control human cytomegalovirus (HCMV) infection, including DNA
38 replication inhibitors such as ganciclovir, and vaccines designed to elicit neutralizing antibodies have had
39 limited success (1, 2), and this may be due in part to the complex genetic diversity of HCMV circulating within
40 human populations (3–9). Basic annotations of the 235kbp HCMV genome identify 165 canonical open
41 reading frames (ORFs), although there is evidence of extensive transcription and translation beyond these loci
42 (10, 11). While nucleotide polymorphisms are found throughout the genome, most sequences are well
43 conserved. 21 of the 165 canonical ORFs show high nucleotide diversity and are distributed as islands
44 throughout the genome. Several groups have reported evidence of frequent recombination within the more
45 conserved regions, which may effectively mix and match the more diverse loci into many different genotype
46 combinations (3, 4, 7, 8). Adding to this complexity, several studies show evidence of gene inactivating
47 mutations (pseudogenes), and gene deletions (7, 8). While some infected individuals may harbor relatively
48 pure populations of HCMV genotypes, complex, multiple genotype infections, and sequential infections by
49 genetically distinct populations also occur. Cloning of HCMV from clinical samples on bacterial artificial
50 chromosomes (BAC) has resulted in numerous, genetically distinct strains for use in laboratory studies. It is
51 not clear how the genetic and phenotypic differences among BAC-cloned HCMV might reflect the natural
52 diversity of HCMV.

53 The glycoprotein (g) H/L complex is functionally conserved among the herpesvirus family and is
54 involved in the initial receptor engagement and the regulation of the membrane fusion protein gB (reviewed in
55 (12)). The HCMV gH/gL is present in the virion envelope as a gH/gL/gO complex (13, 14), a gH/gL/UL128-
56 131 complex (15–18), and in complex with gB (19). Transient expression of HCMV gH/gL and gB is sufficient
57 to drive cell-cell fusion, but is unclear which forms of gH/gL contribute to membrane fusion during HCMV
58 infection (20). The gH/gL/gO and gH/gL/UL128-131 complexes bind to various cell surface receptors through
59 the gO and UL128-131 domains (21–23) and these interactions are important for entry into a broad range of
60 cell types. gH/gL/gO is likely critical for infection of most, or all cell types, fibroblasts, epithelial and
61 endothelial cells being the most extensively studied (24–27). Mutants of HCMV lacking gO are deficient at
62 adsorption, and soluble gH/gL/gO bocks virus adsorption (25, 28). In contrast, gH/gL/UL128-131 is
63 dispensable for infection of fibroblasts and neuronal cells but critical for epithelial and endothelial cells,

64 monocyte-macrophages, and dendritic cells (16, 18, 29–31). Soluble gH/gL/UL128-131 did not block virus
65 adsorption, but there is evidence that engagement of receptors can elicit signal transduction pathways that
66 influence the nature of the resulting infection pathway (21, 28, 30). Murine and guinea pig CMVs contain
67 homologous gH/gL complexes that play similar roles in cell tropism, although there are some differences in
68 the reported requirements for the complexes for infection of different cell types (32–37).

69 We and others have noted striking phenotypic variation among three HCMV strains, TB40/e (TB), TR,
70 and Merlin (ME) in terms of content of the gH/gL complexes in the virion envelope and the corollary effects on
71 entry and cell type tropism. TB and TR contain gH/gL mostly in the form of gH/gL/gO, and very little
72 gH/gL/UL128-131, whereas ME virions contain overall lower amounts of gH/gL and this is mostly in the form
73 of gH/gL/UL128-131 (27). The genetic polymorphism(s) responsible for these differences are unclear.
74 Murrell et al. described a G>T mutation in the UL128 locus of TB that when engineered into ME, reduced the
75 assembly of gH/gL/UL128-131 through effects on mRNA spicing (38). However, this did not fully explain the
76 observed strain differences since TR is also low in gH/gL/UL128-131 but is congenic to ME at this locus (27).
77 Zhang et al. showed that expression of gO during replication is lower in ME-infected cells as compared to TR,
78 but again the genetic correlates of this difference were not clearly identified (39). The cell-free infectivity of
79 HCMV strains on both fibroblasts and epithelial cells correlates with the amounts of gH/gL/gO in the virion
80 envelope; TB is by far the most infectious, followed by TR, while ME virions are poorly infectious (27).
81 Repression of the UL131 promoter in ME resulted in virions with dramatically reduced amounts of
82 gH/gL/UL128-131, somewhat higher levels of gH/gL/gO, and dramatically improved cell-free infectivity (27,
83 40). It seems likely that the low infectivity of cell-free ME at least partially reflects a role for gH/gL/gO in virion
84 adsorption (25, 28).

85 HCMV can spread through monolayer cell cultures by diffusion of cell-free virus in the culture
86 supernatant or by a more cell-associated mode, but the mechanistic distinctions between these modes of
87 spread are not well characterized. Strains vary with respect to their apparent cell-free and cell-associated
88 nature. ME spreads with a characteristic cell-associated pattern whereas TB shows more cell-free spread
89 (40, 41). While this basic observation can be explained by the respective low and high infectivity of ME and
90 TB virions described above, it is not clear how strains compare in their ability to spread by cell-associated
91 modes, nor are the genetic correlates of cell-associated spread well defined. Multiple reports have monitored

92 foci size in the presence of neutralizing antibodies and attributed the cell-associated nature of ME to the
93 expression of the UL128-131 and RL13 loci (24, 42). It seems clear that either gH/gL/gO or gH/gL/UL128-131
94 is required for cell-associated spread on fibroblasts, whereas gH/gL/UL128-131 seems to be required for cell-
95 associated spread in epithelial or endothelial cells (24, 26, 43, 44). Moreover, the pathway of cell-associated
96 spread for HCMV has not been extensively studied. There have been suggestions of limited fusion between
97 infected and uninfected cells allowing the transfer of subviral components, but the efficiency of these
98 processes to facilitate the spread of HCMV infection is not clear (45–47). Syncytium formation has been
99 observed in HCMV infected cultures, but it is not clear whether these cell-cell fusions contribute to viral
100 spread, or merely represent the coalescence of late-stage infected cells long after progeny virus has exited
101 and spread to adjacent cells (48, 49). Here, we report the use of flow cytometry to compare the spread of
102 HCMV TB, TR, and ME in fibroblasts and epithelial cells. The results showed that these strains are specialists
103 for either the cell-free or the cell-associated modes, and that this specialization is not determined by the
104 UL128-131 and RL13 loci.

105 **RESULTS**

106 **HCMV strains exhibit differences in focal pattern and spread efficiency in fibroblasts and**
107 **epithelial cell cultures.** We previously described dramatic differences among BAC-cloned HCMV strains TB,
108 TR, and ME in the levels of gH/gL complexes displayed on the virion envelope, and the corollary effects on
109 infectivity of extracellular virions, which impact the cell-free mode of spread (27, 39, 50). To extend
110 comparative analyses to include both cell-free and cell-associated modes of spread, visual patterns of focal
111 growth were documented under conditions where either mode of spread was accessible. Cultures of
112 fibroblasts or epithelial cells were infected at low multiplicities with GFP-expressing TB, TR, or ME, and
113 spread through the cultures was monitored by fluorescence microscopy over 18 days (Fig 1). In fibroblasts,
114 the spread of all three strains was localized to small, tight foci for up to 12 dpi. By day 18, TB and TR foci
115 were larger and more diffuse, whereas ME foci remained smaller and more localized (Fig 1A). In contrast,
116 foci of all three strains in epithelial cells were more similar to one another throughout the experiment, smaller
117 and more tightly localized than in fibroblasts (Fig. 1B). The diffuse appearance of TB and TR foci on
118 fibroblasts suggested efficient cell-free spread whereas the localized ME foci suggested a more cell-

119 associated mode of spread on these cells. In contrast, all three strains appeared more cell-associated in
120 epithelial cultures.

121 For quantitative comparisons of spread, experiments similar to those described for Figure 1 were
122 performed, but instead of microscopy, flow cytometry was used to measure the number of infected (GFP-
123 expressing) cells over time (Fig 2). In fibroblasts, the number of infected cells for both TB and TR increased
124 exponentially over 12 days, and fit well to a log-linear regression, indicating a constant rate of spread over the
125 course of the experiment (Fig 2A, B). In contrast, ME spread somewhat faster between days 3 and 6, and
126 slower between days 9 and 12. Despite, average spread rates (LN GFP+ cells/day), as indicated by the
127 regression slopes (m), were within 1.2-fold among strains (Fig. 2C). Spread rates for all three stains were
128 lower in epithelial cells than in fibroblasts, and the strains were more different form one another. ME was
129 approximately 2-fold faster than TR and 1.5 fold faster than TB (Fig 2D-F). While differences in the average
130 spread rate among strains on either cell type were small, they were statistically significant (one-way ANOVA:
131 fibroblast, $p=0.0176$; epithelial, $p <0.0001$).

132 **HCMV strains have strong preferences towards either cell-free or cell-associated modes of**
133 **spread.** To assess the contribution of cell-free and cell-associated virus to the observed spread
134 characteristics, the quantity and infectivity of progeny virus in fibroblast and epithelial cell cultures was
135 determined (Fig 3 and 4). Note that since these experiments were intended to correlate with the spread
136 characterizations described above, infectivity of fibroblasts-derived virus was determined on fibroblasts
137 cultures, and infectivity of epithelial-derived virus was determined on epithelial cell cultures.

138 In fibroblasts, TB, TR, and ME generated similar numbers of progeny genomes both within the cells
139 and in culture supernatants (Fig 3A and C). This suggested that DNA replication, nucelocapsid assembly, and
140 egress pathways in these cells were comparable for all three strains. In contrast, the specific infectivity of the
141 progeny was dramatically different among strains. For the cell-free progeny, TB was the most infectious with
142 specific infectivity of approx. 40 genomes per infectious unit (IU), TR was over 100-fold less infectious (6000
143 genomes/IU), and ME was by far the least infectious ($>10^6$ genomes/IU) (Fig. 3B). These comparisons of
144 infectivity were consistent with previous analyses, and were likely due at least in part to the described
145 differences in the levels of gH/gL/gO and gH/gL/UL128-131 (27). Sonication of infected cells was performed
146 to determine the infectivity of cell-associated virus. However, specific infectivity analysis of cell-associated

147 virus was complicated by the fact that a large number of intracellular viral genomes likely remain in the
148 nucleus and are unlikely to contribute to infectivity. Thus, nuclei were removed and the quantity of viral
149 genomes remaining in cytoplasmic fractions was determined. When analyzed in this manner, intracellular
150 virus infectivity resembled that of the cell-free virus with TB the most infectious, followed by TR, and ME was
151 by far the least infectious (Fig 3D).

152 In epithelial cells, the release of cell-free virus was notably different among strains (Figs 4A and C).
153 ME released 80 virions per cell compared to 12 for TB and only 2 for TR (Fig 4A). The specific infectivity of
154 cell-free, epithelial-derived TB (epi-TB) was approximately 600 genomes/IU whereas cell-free epi-TR and epi-
155 ME were 3 and 5-fold less infectious, respectively (TR=1600 genomes/IU; ME=3000 genomes/IU) (Fig 4B).
156 Note that while TB released 6-fold fewer cell-free progeny than ME, the cell-free TB progeny were 5-fold more
157 infectious than the ME progeny (compare Figs 4 A and B). This indicates that TB and ME generate
158 comparable amounts of total infectivity into epithelial cell culture supernatants. In contrast, TR produced far
159 less total cell-free infectivity in these cultures since the low quantity of progeny released was not compensated
160 by better infectivity. The accumulation of epithelial cell-associated progeny was comparable among strains
161 and the cell-associated infectivity was within the range of 15,000-45,000 genomes/IU for all strains (Fig 4C
162 and D.).

163 To further evaluate the contribution of cell-free and cell-associated spread mechanisms, neutralizing
164 antibodies were used with the rationale that they inhibit cell-free spread more potently than cell-associated
165 spread. Neutralizing antibodies chosen for these experiments were mAb 14-4b, which likely targets a
166 discontinuous epitope at the membrane proximal region of gH (51, 52), as well as a mixture of rabbit anti-
167 peptide sera that target UL130 and UL131 (17). The relative potency of these antibodies to neutralize cell-
168 free TB, TR, and ME was verified in neutralization experiments (Fig. S1). Spread rates of each strain in
169 either fibroblast or epithelial cell cultures were then determined in the presence or absence of anti-gH mAb 14-
170 4b or anti-UL130/131 sera at concentrations sufficient for complete neutralization of cell-free virions. To
171 demonstrate that the observed spread required production of progeny viral genomes and was not the result of
172 transfer of cytoplasmic contents from infected to uninfected cells, spread in the presence of ganciclovir was
173 also determined (Fig 6).

174 In fibroblasts, anti-gH 14-4b reduced the spread rate of TB and TR to 30% and 45% of control,
175 respectively (Fig 5 A-B). ME was notably more resistant to mAb 14-4b, with a spread rate of 75% of control
176 (Fig 5 C). This was especially noteworthy since cell-free ME was more sensitive to neutralization than either
177 TB or TR (Fig. S1). Consistent with the dispensability of gH/gL/UL128-131 in fibroblasts, anti-UL130/131 sera
178 had no effect on the spread rates of any of the three strains in fibroblasts (Fig 5, A-C). The residual spread of
179 all strains in the presence of neutralizing antibodies was greater than with ganciclovir treatment, even for TR,
180 which is known to harbor resistance mutations in the UL97 kinase (53). These results support the hypothesis
181 that spread of TB in fibroblasts predominately involved cell-free virions that were sensitive to neutralizing
182 antibodies, whereas ME spread predominately in a manner not sensitive to antibody neutralization (i.e., not by
183 cell-free virions). This interpretation is consistent with the earlier observations that while all strains release
184 similar numbers of cell-free progeny, ME virions are far less infectious, and thus less likely to contribute to
185 efficient cell-free spread (Fig 3). The intermediate antibody sensitivity of TR spread might indicate an
186 intermediate contribution of cell-free and cell-associated spread mechanisms. However, it may also reflect the
187 lack of complete neutralization of cell-free TR (Fig S1).
188 In epithelial cell cultures, the presence of anti-gH 14-4b had no effect on the spread rates for TB, TR,
189 or ME, and anti-UL130/131 had a marginal effect, with a 30% reduction for TR being the largest (Fig 5D-F). If
190 cell-free virus significantly contributed to spread in epithelial cells, inhibition by both anti-gH and anti-
191 UL130/131 would have been expected since both antibodies potently neutralized cell-free virus of all three
192 strains on these cells (Fig S1). This suggests that the observed spread of all strains in epithelial cells
193 predominately involved a cell-associated mode that was resistant to neutralization of cell-free virus. The
194 modest inhibition by anti-UL130/131 may suggest differences in the specific mechanisms blocked by these
195 antibodies compared to anti-gH 14-4b. While both types of antibodies can evidently block cell-free infection,
196 the anti-UL130/131 appears to be able to inhibit the cell-associated mode, albeit less efficiently than they
197 block cell-free infection. This interpretation is consistent with conclusions of Murrell et al. that cell-associated
198 spread of ME may be blocked by antibodies, but less potently (42).
199 In sum, the results of this set of experiments indicate; 1) HCMV can spread in fibroblast cultures with
200 similar efficiencies through either a cell-free mode, exemplified by TB, or a cell-associated mode, exemplified
201 by ME. 2) In APRE19 epithelial cells, spread by all three strains was predominantly cell-associated, but

202 efficiencies varied, ME was by far the most efficient. 3) Efficient cell-free spread (as exemplified by TB in
203 fibroblasts) correlated with the detection of higher quantity and infectivity of cell-free progeny in culture
204 supernatants. Conversely, efficient cell-associated spread (exemplified by ME in either fibroblasts or epithelial
205 cells) did not correlate with the quantity or infectivity of cell-associated progeny in cell sonicates.

206 **The specialization to cell-associated spread of HCMV ME is not determined by high levels of**
207 **gH/gL/UL128-131.** The cell-associated nature of ME has been linked to the high expression levels of UL128-
208 131 and the corollary poor infectivity of cell-free ME virions (24, 27, 40, 42). To address this in our
209 quantitative system, we made use of the previously described tetracycline (Tet)-repression system developed
210 by Stanton et al. (40). Briefly, the BAC clone of ME used in these studies contained tetracycline-operator
211 (TetO) sequences in the promoter of UL131. We previously showed that replication of this recombinant ME in
212 fibroblasts expressing the tetracycline-repressor (TetR) protein produced extracellular virus with amounts of
213 gH/gL/UL128-131 at or below that of TB and TR, marginally higher amounts of gH/gL/gO, and these changes
214 in glycoproteins greatly improved cell-free infectivity (27). In order to test the role of high UL128-131
215 expression for ME spread, experiments were conduced using these TetR-expressing fibroblasts (HFFFtet), as
216 well as a newly generated TetR-expressing ARPE19 epithelial cell line (ARPEtet). Both HFFFtet and ARPEtet
217 showed efficient repression of a TetO-regulated luciferase reporter (Fig. 6A). Consistent with our previous
218 characterizations, ME virions produced in HFFFtet cells contained drastically reduced amounts of
219 gH/gL/UL128-131, increased gH/gL/gO, and infectivity was dramatically improved (Fig 6B and C). Similarly,
220 ME virions produced in ARPEtet cells contained dramatically reduced amounts of gH/gL/UL128-131
221 compared to virions from control ARPE cells, but did not contain increased gH/gL/gO, or display enhanced
222 infectivity as was observed for fibroblasts-derived virus (Fig 6B). Note that even without repression of
223 gH/gL/UL128-131, the specific infectivity of epi-ME on epithelial cells was dramatically better than fib-ME on
224 fibroblasts (Fig 6C).

225 In fibroblasts, gH/gL/UL128-131 repression did not influence spread rates or the sensitivity of spread to
226 neutralizing antibodies (Fig 7A). Thus, the efficient cell-associated spread of ME in fibroblasts does not
227 require high levels of gH/gL/UL128-131. In epithelial cells, repression of gH/gL/UL128-131 resulted in a
228 modest decrease in average spread rate (from 0.38 to 0.29), and small increase in the sensitivity of spread to
229 anti-UL130/131, (from 10% to 30% inhibition) (Fig 7B). The reduction in spread was consistent with the

230 important role of gH/gL/UL128-131 for HCMV in these cells. On the other hand, the increase in antibody
231 sensitivity was more complicated to interpret. One possibility is that this reflected a shift towards increased
232 cell-free spread. This seems unlikely since repression of gH/gL/UL128-131 did not enhance cell-free
233 infectivity (Fig 6). Alternatively, it may be that reduced gH/gL/UL128-131 expression allowed for more efficient
234 blocking of the cell-associated spread by these antibodies. In any case, ME spread in ARPEtet cells was still
235 highly resistant to antibodies as compared to the spread of TB in fibroblasts (compare 30% antibody resistant
236 spread for TB in fibroblasts; Fig 5A, to 70% resistant for ME in ARPEtet; Fig 7B). Overall, these results
237 indicated that while reduction of gH/gL/UL128-131 may enhance cell-free modes of spread, at least on
238 fibroblasts, high expression levels of the gH/gL/UL128-131 could not explain the highly specialized cell-
239 associated spread of ME.

240 **Spread inhibition due to RL13 expression is more pronounced in fibroblasts than in epithelial**
241 **cells, and influences both cell-free and cell-associated modes of spread.** The RL13 ORF encodes an
242 envelope glycoprotein that has been described as an inhibitor of HCMV replication in culture and mutations in
243 RL13 have been documented during cell-free passage in fibroblasts and epithelial cells (40, 54, 55). While
244 the ME recombinant used in the present studies harbors such a RL13 mutation, the RL13 expression status of
245 the TB and TR BAC-clones is unclear. Both TB and TR have intact RL13 ORFs confirmed by DNA
246 sequencing, but lack of quality antibodies makes protein detection difficult. To compare the effect of RL13 on
247 the spread of all three strains, and to avoid potential selection of RL13 mutants during spread experiments,
248 fibroblast and epithelial cell lines that express RL13 were engineered. Immunoblot analysis demonstrated that
249 these cell lines expressed of both mature and immature proteoforms, and flow cytometry confirmed similar
250 expression levels (Fig S2). The effects of RL13 expression on spread rates, and the quantity and infectivity of
251 cell-free and cell-associated progeny virus were then analyzed (Fig 8).

252 In fibroblasts, RL13 expression resulted in a comparable 40-50% reduction in spread rate for all three
253 strains (Fig 8A). Inhibition of spread by neutralizing antibodies was not affected for TB or TR, but spread of
254 ME in RL13 expressing cells was approximately 50% more sensitive than in control cells (Fig 8B). These
255 observations could not be universally explained by effects on progeny virus production since effects of RL13
256 expression on these parameters were generally small and varied among strains (Fig 8C). Moreover, the only

257 statistically significant change in progeny infectivity due to RL13 expression was observed for cell-free TB,
258 which was 6-fold less infectious than virus produced from control fibroblasts (Fig. 8D).

259 In epithelial cells, RL13 expression reduced spread by approximately 20% for all three strains, but this
260 only reached statistical significance in the case of ME (Fig 8E). Spread of TB was notably more sensitive to
261 antibody inhibition, whereas TR and ME were less affected (Fig 8F). As in fibroblasts, these effects were not
262 readily attributable to the quantity or infectivity of progeny since 1) there were no significant changes to the
263 quantity of cell-associated or cell-free progeny virus for any of the three strains (Fig 8G), and 2) the only
264 notable effect on progeny infectivity was in the case of cell-free ME, which was 120-fold less infectious when
265 produced in RL13-expressing epithelial cells as compared to control cells (Fig. 8H).

266 To determine if the observed reduction in infectivity of cell-free ME produced in RL13 expressing
267 epithelial cells was related changes in the virion content of gH/gL complexes or gB, equal quantities of
268 fibroblast- or epithelial-derived extracellular virions of ME were subjected to non-reducing SDS-PAGE and
269 immunoblot analysis with antibodies specific for gL to detect gH/gL complexes, or with anti-gB monoclonal
270 antibodies that react with both the full length 165-170 kDa form and the 55 kDa portion of the furin-cleaved
271 form of gB (56–58) (Fig 9). Fib-ME virions contained gH/gL primarily in the form of gH/gL/UL128-131, and
272 most of the gB was in the furin-cleaved form. RL13 expression in fibroblasts seemed to have little effect on
273 either gH/gL complexes or gB. However, there were notable differences in epithelial cells. First, epi-ME
274 virions contained greater amounts of gH/gL/UL128-131 than fib-ME, and this was somewhat reduced by RL13
275 expression. Secondly, epi-ME had more uncleaved gB, whereas ME virions produced by RL13 expressing
276 epithelial cells had less overall gB, and it was mostly furin-cleaved. Together, these results indicated that the
277 processing and incorporation of gH/gL complexes and gB into cell-free progeny can be influenced by the cell
278 type, and in epithelial cells, this may be further affected by RL13 status. While the effects on gB seem to
279 correlate with the observed reduction in ME infectivity in RL13 epithelial cells, a strong causal connection
280 would be a premature conclusion.

281 In sum, these results indicate that 1) RL13 expression tempers the spread of HCMV in fibroblasts by
282 either the cell-free mode exemplified by TB, or the cell-associated mode exemplified by ME, 2) The effect of
283 RL13 on spread in epithelial cells is less dramatic than in fibroblasts, 3) effects of RL13 on progeny production
284 and release from either cell type are generally small, and 4) RL13-expression in epithelial cells dramatically

285 reduces the infectivity of cell-free ME progeny, and this is coincident with changes in gH/gL complexes and
286 gB.

287 **DISCUSSION**

288 Distinctions between cell-free and cell-associated phenotypes of HCMV strains have been noted, but
289 the mechanistic differences, and the genetic loci involved in these modes of spread remain to be understood.
290 Sinzger et al. showed that during the initial rounds of cell-associated subculturing in fibroblasts, clinical HCMV
291 isolates formed small and tightly packed foci, but tended towards larger and more diffuse foci during later
292 rounds of passage (59). The change in foci morphology coincided with the appearance of infectious virus in
293 culture supernatants and the basic interpretation was that the adaptation of clinical HCMV to the cell culture
294 environment involved a shift from cell-associated to cell-free modes of spread. A more recent report by
295 Galitska et al. noted variation in clinical HCMV samples, with some displaying the characteristic small foci, but
296 others showing larger diffuse foci even in early rounds of subculturing (60). This variation fits well with the
297 notion of genotypic diversity of HCMV populations within clinical specimens (3, 4, 6, 8, 9) and the earlier
298 suggestion by Sinzger et al. that the observed culture adaptation of HCMV clinical isolates might represent
299 random sampling or purifying selection of preexisting genotypic variants, rather than the acquisition of *de novo*
300 mutations (59). In line with this view, Subramanian et al. used a flow cytometry method to determine the
301 increase in HCMV infected cells over time to better quantitate spread kinetics and found that some low
302 passage clinical isolates spread more rapidly than others (61). They interpreted slow kinetics to represent a
303 cell-associated-only phenotype and fast kinetics to represent a phenotype of both cell-associated and cell-free
304 spread. Indeed, the faster spreading isolates were more sensitive to the presence of neutralizing antibodies.
305 Together, these and other studies suggest considerable variation in the modes of spread exhibited by
306 genetically distinct HCMV, but the exact genetic variations that determine these phenotypes remain unclear.

307 Here we applied a flow cytometry-based approach to compare the spread characteristics of three
308 commonly studied and genetically distinct BAC clones of HCMV, TB, TR and ME in both fibroblast and
309 epithelial cell cultures. In addition to measuring the rates of spread in the presence or absence of neutralizing
310 antibodies, we also characterized the quantity and infectivity of cell-free and cell-associated progeny
311 produced. TB and ME markedly preferred cell-free and cell-associated modes of spread, respectively,
312 whereas TR seemed to be overall less efficient. While either mode could suffice for efficient spread in

313 fibroblast cultures, spread in epithelial cell cultures seemed generally skewed towards a cell-associated mode.
314 Consistent with this, ME demonstrated more efficient spread in epithelial cells than either TB or TR. Finally,
315 while the efficiency of cell-free spread correlated with the abundance and infectivity of progeny virus released
316 to culture supernatants, the efficiency of cell-associated spread did not correlate with cell-associated
317 infectivity. In both cell types, ME was far more efficient at cell-associated spread than TB or TR, but did not
318 produce more cell-associated infectivity as measured by titration of sonicated infected cells. This suggests
319 that the efficient cell-associated spread mechanism of ME depends on the intact cell monolayer. Moreover, it
320 seems logical that the poor infectivity of ME virions would be highly detrimental to efficient cell-free spread,
321 whereas cell-associated mechanisms might be less sensitive to poor infectivity. On the other hand, it seems
322 unlikely that the log-folds better infectivity of TB and TR virions would be detrimental to the efficiency of cell-
323 associated spread by these strains (Fig 10). Thus, it seems that ME has a specific mechanism(s) to enhance
324 cell-associated spread that does not depend on production of highly infectious virions. The mechanisms
325 driving the highly efficient cell-associated spread of ME remain unclear, but have been suggested to involve
326 the functions of gH/gL/UL128-131 and RL13 (24, 40, 42, 62).
327 Our finding that the level of gH/gL/UL128-131 expression did not affect the spread rate of ME in
328 fibroblasts conflicts with Stanton et al., which showed UL128-null ME plaques significantly larger than UL128-
329 intact ME plaques (40). The apparent contradiction may be explained by the fact that our flow cytometry
330 assays measured spread rates averaged over 12 days as compared to the measurements of 21 day plaque
331 sizes by Stanton et al. Linear regression analyses of the data collected by flow cytometry indicated that ME
332 spread at a faster rate between days 3 and 6, and then began to slow after day 9 (Figure 2). This slowdown
333 likely reflects the limiting number of potential uninfected target cells available via cell-associated spread during
334 focal expansion. Contrast this with the constant rates of TB and TR spread, likely indicative of unlimited
335 potential uninfected target cells available via diffusion of progeny virus throughout the culture supernatant.
336 Thus, the increase in 21 day plaque size of a UL128-null ME documented by Stanton is consistent with
337 enhanced cell-free infectivity, but our analysis of spread rate over 12 days indicates this does not come at the
338 expense of a distinct and comparably efficient mode of cell-associated spread. This interpretation is
339 supported by the observation that the 12 day spread rate was highly resistant to neutralizing antibodies
340 regardless of gH/gL/UL128-131 expression level (Fig 8) and is consistent with Laib Sampaio et al. who

341 showed much greater cell-free dispersion of UL128-null ME foci, but more similar antibody resistant, cell-
342 associated spread with or without UL128 (24). In epithelial cells, repression of gH/gL/UL128-131 did reduce
343 the 12 day spread rate for ME (Fig 8). This was consistent with reduced plaques sizes of UL128-null ME
344 documented by Murrell et al., and likely reflects the important role of gH/gL/UL128-UL131 in epithelial cells
345 (38). However, as observed in fibroblasts, spread in epithelial cells was still highly resistant to neutralizing
346 antibodies when gH/gL/UL128-131 was repressed. This was different than Murrell et al. who concluded that
347 spread of ME in epithelial cells was more sensitive to antibodies when gH/gL/UL128-131 was reduced (42).
348 Again the discrepancy likely reflects that analysis of 21-day plaque size likely accentuates the effects of cell-
349 free infectivity and masks the contribution of cell-associated spread. Thus, by measuring average spread
350 rates over 12 days, we find that gH/gL/UL128-131 levels do not determine the cell-free versus cell-associated
351 spread phenotype for ME on either fibroblasts or epithelial cells.
352 The RL13 glycoprotein was another candidate for a factor influencing the cell-free and cell-associated
353 phenotypes. Previous reports, using a number of different approaches, concluded that expression of RL13
354 limits HCMV replication in both fibroblast, epithelial, and endothelial cell cultures (24, 40, 54, 55). Our results
355 are in general agreement with these reports, and also demonstrate some variability in the effects of RL13 with
356 respect to the HCMV strain and the cell type. For each of the strains TB, TR, and ME, RL13 expression
357 reduced spread in fibroblasts more substantially than in epithelial cells. In the case of TB on fibroblasts,
358 RL13 expression reduced the release of cell-free progeny, but this effect was less pronounced for TR or ME
359 on fibroblasts, and there was no effect on cell-free progeny release in epithelial cells for any strain.
360 Interestingly, RL13 expression dramatically reduced the infectivity of cell-free virions released by ME from
361 epithelial cells, and this was consistent with results of Stanton et al. showing low cell-free titers for RL13-intact
362 ME in epithelial cell cultures compared to RL13 mutant ME (40). The physiological basis of this effect on ME
363 infectivity remains unclear, but it seemed to correlate with differences in gH/gL complex and gB incorporation.
364 Epi-ME virions contained more gB than fib-derived ME virions and much of the elevated gB was in the
365 uncleaved form. Strive et al. showed that furin cleavage was not required for the function of HCMV gB (63).
366 Therefore, the increased levels of gB in epi-ME may partly explain the increased infectivity relative to fib-ME.
367 RL13 expression in epithelial cells reversed both the increase in uncleaved gB and reduced virion infectivity.
368 Finally, RL13 expression did not appear to promote cell-associated spread since the sensitivity of spread to

369 neutralizing antibodies in RL13-expressing cells was either unaffected or marginally increased for all three
370 strains. Thus, RL13 seems to dampen one or more aspects of HCMV replication that can manifest through
371 either mode of spread. The specific effects of RL13 may vary depending on other physiologic differences
372 between strains and cell types.

373 Mutational inactivation of the UL128-131 and RL13 loci during serial propagation of HCMV in culture is
374 a phenomenon that has been universally ascribed to HCMV, despite clear strain variably. While ME is highly
375 sensitive to the selection of *de novo* UL128-131 in fibroblast cultures, TB and TR are remarkably stable in this
376 respect (40, 55, 59). This disparity might simply indicate that many subculturing methods, including
377 supernatant transfer, cell sonication, and high split-ratio transfer of intact infected cells, would be expected to
378 heavily favor cell-free spread. Thus, given the highly efficient cell-associated spread of ME described in the
379 analyses presented here, propagation by low split-ratio passage of intact, infected cells might reduce the
380 selective bottleneck on UL128-131 function for efficient cell-associated spreaders like ME. RL13 inactivating
381 mutations have also been reported for many strains and clinical isolates in studies involving fibroblasts,
382 epithelial, and endothelial cells (10, 54). The BAC clones of TB and TR have intact RL13 ORFs, but since
383 expression of RL13 from transduced cells reduced replication by these strains, it may be that both strains
384 contain mutations or polymorphisms in the signal peptide, or other regulatory sequences, that impact RL13
385 expression. Moreover, our results suggest that the selection against RL13 may be more extensive in
386 fibroblasts but less pronounced in epithelial cells. Notably, a recent report by Ourahmane et al. showed that
387 the presence of neutralizing antibodies during subculturing of clinical urine-derived HCMV in fibroblasts
388 stabilized the UL128-131 and RL13 loci in the resultant virus populations (62). If these clinical isolates were
389 similar to ME in their proclivity for cell-associated spread, (note that ME was also isolated from a urine sample
390 (10)), it would seem logical that neutralizing antibodies would reduce the selective advantage of cell-free
391 infectivity conferred by UL128-131 mutation. The preservation of RL13 is less intuitive since RL13 seems to
392 impact both cell-free and cell-associated modes of spread. However, given the variable effects we observed
393 of RL13 on different strains, these observations may point to epistasis phenomena, where the relative effect of
394 any given perturbation at one variable locus is influenced by variable physiology related to other polymorphic
395 loci.

396 Our data also shed new light on the idea that the cell type might influence phenotypic properties in a
397 non-genetic manner through changes to the protein composition of the progeny virus. Among the
398 herpesviruses, these so called "producer cell effects" have been particularly well characterized for EBV, where
399 the mechanism alternates the tropism of progeny virus between epithelial and B-cells (reviewed in (64)).
400 Scrivano et al. suggested a similar phenomenon for HCMV based in part on data showing that progeny virus
401 produced from endothelial cells had less UL128 protein in the envelope compared to fibroblast derived
402 progeny (35). This is in stark contrast to our results that epithelial-derived HCMV contained greater amounts
403 of gH/gL/UL128-131 than fibroblast-derived virus (Fig 9). There are several possible, non-mutually exclusive
404 explanations for this discrepancy. This could reflect differences between strains as the Scrivano et al.
405 experiments used TB, whereas our analyses used ME only since the production of TB and TR from epithelial
406 cells was too low to allow immunoblot analyses for these strains. There could also be differences between
407 endothelial and epithelial cells. Finally, the Scrivano et al. analysis normalized virion immunoblots to gB,
408 whereas we used major capsid protein (MCP). It is possible that incorporation of gB into progeny virus is
409 affected by glycoprotein processing/secretory pathway differences between cell type, whereas plasticity in the
410 number of capsid subunits per virion seems less likely. Indeed, we observed differences in the proteolytic
411 processing and virion incorporation of gB when ME was produced in fibroblast and epithelial cells.
412 Nevertheless, Scrivano et al. also noted an apparent change in the relative fibroblast versus endothelial
413 tropism depending on nature of the producer cell. While we observed differences in infectivity between
414 fibroblast and epithelial cell derived virus, it is important to note that our analyses involved congruent cell
415 types to correspond with the observed kinetics of viral spread in monolayer cultures. Questions regarding the
416 spread of HCMV between cell types were outside the scope of the present studies.
417 In conclusion, we have characterized very different cell-free and cell-associated spread phenotypes
418 among three commonly studied BAC clones of HCMV. It seems likely that these phenotypic variances are
419 manifest through the combined influences of diversity at multiple genetic loci other than UL128-131 and RL13.
420 How this phenotypic variation is represent *in vivo* remains unclear. There is little clear evidence to support the
421 notion that HCMV is predominately cell-associated *in vivo*. The endemic nature, and the pleomorphic
422 disseminated disease presentations suggest that HCMV is able to thrive in many different bodily environments
423 as it spreads within and among individual human hosts. Copious amounts of cell-free virus are shed in urine,

424 saliva, and breast milk, and this is likely a major route of transmission between individuals, whereas HCMV in
425 the blood is likely highly associated with leukocytes (65–67). Thus, it seems likely that both cell-free and cell-
426 associated modes of spread are important to the natural history of HCMV.

427 **MATERIALS AND METHODS**

428 **Cell lines.** Primary neonatal human dermal fibroblasts (nHDF; Thermo Fisher Scientific), RL13-nHDFs
429 (nHDFs transduced with lentiviral vectors encoding RL13 of HCMV strain Merlin, selected with puromycin
430 resistance), MRC-5 fibroblasts (American Type Culture Collection; CCL-171), and HFFF-tet (40) (provided by
431 Richard Stanton, Cardiff University, United Kingdom) were grown in Dulbecco's modified Eagle's medium
432 (DMEM)(Sigma) supplemented with 6% heat-inactivated fetal bovine serum (FBS) (Rocky Mountain
433 Biologicals, Missoula, MT, USA) and 6% Fetalgro® (Rocky Mountain Biologicals, Missoula, MT, USA).
434 Retinal pigment epithelial cells (ARPE19)(American Type Culture Collection, Manassas, VA, USA), ARPE-tet
435 (ARPE19 cells transduced with retroviral vectors encoding the tetracycline repressor protein, and selected by
436 puromycin resistance), and RL13-ARPE (transduced with lentiviral vectors encoding RL13 of HCMV strain
437 Merlin, selected with puromycin resistance) were grown in a 1:1 mixture of DMEM and Ham's F-12 medium
438 (DMEM:F-12)(Gibco) and supplemented with 10% FBS.

439 **Retro- and lentiviral vectors.** The Tet repressor protein bearing a nuclear localization signal was extracted
440 by PCR from the integrated sequence in the HFFF-tet chromosomal DNA and cloned into the same pMXs
441 retrovirus vector used to construct HFFF-tet (40). The pMXs retrovirus vector plasmid was a gift from Dr.
442 Toshio Kitamura at the Institute of Medical Science, University of Tokyo (68). The tet-containing vector
443 plasmid was transformed in 293T cells together with the pUMVC and pMD2.G helper plasmids. The pUMVC
444 helper plasmid was a gift from Bob Weinberg (Addgene plasmid # 8449) (69). Two days after transformation,
445 the retroviral particles in the supernatant were purified from cell debris thru syringe filtration and centrifugation.
446 After titration, the particles were used to transduce low passage ARPE-19 cells. After a week of puromycin
447 selection, cells aliquots were tested for tetR expression after transfection of a firefly luciferase tetR-reporter
448 system and aliquots were stored in liquid nitrogen until further usage. The codon-optimized RL13 with an
449 intact ORF from Merlin HCMV strain (NCBI ref YP_081461) was constructed by Gibson Assembly and used to
450 replace the eGFP ORF in the pLJM1-EGFP lentiviral transfer vector plasmid. The pLJM1-EGFP plasmid was
451 a gift from David Sabatini (Addgene plasmid # 19319) (70). The RL13-containing vector plasmid was

452 transformed in 293T cells together with three lentiviral helper plasmids. The pMDLg/pRRE, pRSV-Rev, and
453 pMD2.G helper plasmids were a gift from Didier Trono (Addgene plasmids # 12251, # 12253, # 12259,
454 respectively) (71). Two days after transformation, the lentiviral particles in the supernatant were purified from
455 cell debris thru syringe filtration and centrifugation. After titration, the particles were used to transduce either
456 low passage nHDF or ARPE-19 cells. After a week of puromycin selection, cells were tested for RL13
457 expression and aliquots were stored in liquid nitrogen until further usage.

458 **HCMV.** All human cytomegalovirus (HCMV) strains were derived from bacterial artificial chromosome (BAC)
459 clones. BAC clone TB40/e (BAC4) was provided by Christian Sinzger (University of Ulm, Germany) (41).
460 BAC clone TR was provided by Jay Nelson (Oregon Health and Sciences University, Portland, OR, USA) (72).
461 BAC clone Merlin (ME)(pAL1393), which contains tetracycline operator sequences within the transcriptional
462 promoter of UL130 and UL131, was provided by Richard Stanton (Cardiff University, Cardiff, United Kingdom)
463 (40). All BAC clones were modified to express green fluorescent protein (GFP) with En passant
464 recombineering (73) by replacing US11 with the eGFP gene. The constitutive expression of eGFP allows the
465 monitoring of HCMV infection early and is strain-independent. Infectious HCMV was recovered by
466 electroporation of BAC-DNA into HFFFs, as previously described (26). For infectious unit (IU) determination,
467 viruses were serial diluted and infectivity was determined on fibroblasts or epithelial cells using flow cytometry
468 48 hours post infection.

469 **Antibodies.** Monoclonal antibodies specific to HCMV major capsid protein (MCP), gH (14-4b), and gB (27-
470 156) were provided by Bill Britt (University of Alabama, Birmingham, AL) (51, 57, 74). 14-4b was purified by
471 FPLC prior to use. Rabbit polyclonal sera against HCMV gL, UL130, and UL131 were provided by David
472 Johnson (Oregon Health and Sciences University, Portland, OR) (17).

473 **Vrial spread assays.** Approx. $1x10^5$ ($3x10^5$) nHDFs (ARPEs) were seeded into 6-well culture plates and
474 allowed to grow to confluence. Confluent monolayers of nHDFs or ARPE cells were inoculated with 100-1000
475 IUs of strains TB, TR, or ME at for 4hrs at 37°C. Cells were then washed extensively with PBS and cultured in
476 the appropriate growth medium supplemented with 2% FBS. Viral spread in the presence or absence of
477 neutralizing antibodies or ganciclovir was monitored over 12 days by flow cytometry. All experiments were
478 performed in triplicate and a minimum of 3 experiments was conducted for each condition. Spread rates were

479 determined by plotting LN GFP+ cells over time and fitting the data to the log-linear rate expression $LN(I)_t$ =
480 $m(t) + LN(I)_0$ where (I) is the number of GFP+ cells, (t) is the time in days, and *m* is the spread rate.

481 **Flow cytometry.** Recombinant GFP-expressing HCMV-infected cells were washed twice with PBS and lifted
482 with trypsin. Trypsin was quenched with DMEM containing 10% FBS and cells were spun at 500xg for 5 min
483 at RT. Cells were fixed in PBS containing 2% paraformaldehyde for 10 min at RT, then washed and
484 resuspended in PBS. Samples were analyzed using an AttuneNxT flow cytometer. Cells were identified
485 using FSC-A and SSC-A, and single cells were gated using FSC-W and FSC-H. BL-1 laser (488nm) was
486 used to identify GFP+ cells, and only cells with median GFP intensities 10-fold above background were
487 considered positive. RL13 expression was measured using an intracellular staining kit (Thermo) and an anti-
488 6His antibody conjugated to AlexaFluor-647 using the RL-2 laser (647nm).

489 **qPCR.** The real time quantitative PCR (qPCR) assay used to quantify viral or cellular DNA molecules was
490 performed as previously described (27). Briefly, HCMV DNA inside cell-free particles was purified using the
491 PureLink Viral RNA/DNA mini kit (Thermo Scientific). A region within UL83 conserved among ME, TR, and
492 TB was chosen as the HCMV-specific amplicon, and viral genomes were quantified by SYBR green qPCR as
493 previously described. Standard curves were performed using serial dilutions of a single PCR DNA band
494 containing the sequences of the viral UL83 and cellular beta2-microglobulin (see below) amplicons and the
495 corresponding set of primers. Finally, the concentration of HCMV DNA genomes in the supernatant was
496 extrapolated from the UL83 standard curve and expressed as genome molecules per ml of media
497 (genome/ml). Total intracellular or cytoplasmic HCMV DNA was quantified with the UL83-based qPCR after
498 extracting viral and cellular DNA from infected cells with the PureLink Genomic DNA mini kit (Thermo
499 Scientific). We also measured the chromosomal DNA molecules present in these samples with an amplicon
500 located in the human beta-2 microglobulin gene (75). These chromosomes numbers were used to correct for
501 the number of cells when measuring the specific infectivity of cell-associated HCMV particles from different
502 samples. To that purpose, another aliquot of infected cells was first subjected to a Subcellular Fractionation
503 Kit for cultured cells (Thermo Scientific) to purify the cytoplasmic HCMV particles from the excess of nuclear
504 HCMV DNA. Lastly, genomes present in the cytoplasmic fraction were purified using the Genomic DNA mini
505 kit and their number was measured with the UL83-based qPCR assay.

506 **Particle production.** Production of intracellular and extracellular HCMV genomes was determined over a
507 time course of 4 days. Briefly, nHDFs and ARPEs were infected with HCMV strains TB, TR, or ME at an MOI
508 of 1, and the cells were extensively washed 3 days post infection. At 3, 5, and 7 dpi culture supernatants
509 were collected and spun at 500xg for 10 minutes at RT, while cells were lifted with trypsin and then quenched
510 with culture media containing 10% FBS. Cells were spun at 500xg and resuspended into aliquots. Cells were
511 either resuspended in PBS for whole cell analysis, fractionated for specific infectivity analysis, sonicated to
512 release cell-associated virus, or processed for flow cytometry to determine the number of infected cells. The
513 number of HMCV genomes in the whole cell and supernatant was measured by qPCR, normalized to load,
514 and divided by the number of GFP+ cells. For specific infectivities, the number of HCMV genomes per mL in
515 the supernatant or cytoplasmic fractions was divided by the IUs per mL of the supernatants and cell sonicates.
516 The accumulation at day 7 from nHDFs and ARPEs is shown in Fig 3 and 4, respectfully.

517 **Immunoblot analyses.** Cell-free virions were solubilized in a buffer containing 20mM Tris-buffered saline
518 (TBS) (pH 6.8) and 2% SDS. Protein samples were separated by SDS-polyacrylamide gel electrophoreses
519 (SDS-PAGE) and electrophoretically transferred to polyvinylidene difluoride membranes in a buffer containing
520 10mM $NaHCO_3$ and 3mM Na_2CO_3 (pH 9.9) and 10% methanol. Transferred proteins were first probed with
521 MAbs or rabbit sera, then anti-mouse or anti-rabbit secondary antibodies conjugated to horseradish
522 peroxidase (Sigma), and Pierce ECL-Western Blotting substrate (Sigma). Chemiluminescence was detected
523 using a Bio-Rad ChemiDoc MP imaging system.

524 **ACKNOWLEDGEMENTS**

525 We are grateful to Richard Stanton, Bill Britt, Jay Nelson, and David Johnson, for generously supplying
526 HCMV BAC clones, antibodies, and cell lines as indicated in the Materials and Methods. Additionally, we are
527 grateful to the Center for Biomolecular Structure and Dynamics (CBSD), University of Montana, Missoula, MT,
528 for purification of monoclonal antibodies, and well as the Flow Cytometry Core of the Center for Environmental
529 Heath Sciences (CEHS), University of Montana, Missoula, MT, for guidance on experimental design,
530 acquisition, and analysis of the flow cytometry-based approaches used for this study.

531 Experiments were designed by E.P.S, B.J.R, and J.L., and performed by E.P.S, J.L, L.Z.D., C.P., J.P,
532 and Q.Y., and the manuscript was prepared by B.J.R., E.P.S., and J.L.

533 **FIGURE LEGENDS**

534 **Fig 1. Comparison of focal spread patterns of distinct HCMV stains.** Confluent monolayers of fibroblasts
535 (A) or epithelial cells (B) were infected at an MOI of 0.001 with GFP-expressing HCMV strains TB, TR, or ME.
536 Foci were documented by fluorescence microscopy at 6, 12, and 18 days post infection. Four representative
537 fields (10X) are shown for each.
538 **Fig 2. Quantitation of HCMV spread by in fibroblasts and epithelial cells.** Confluent 6cm monolayers of
539 fibroblasts (A) or epithelial cells (D) were infected with 1000 IUs of GFP-expressing HCMV strains TB, TR, or
540 ME. The number of infected cells at 3, 6, 9, and 12 days post infection was determined by flow cytometry. To
541 determine exponential growth rates, the LN GFP+ cells is plotted at each time point for fibroblasts (B) and
542 epithelial cells (E). The average spread rates (LN GFP+ cells per day) of the three strains were determined
543 for fibroblasts (C) and epithelial cells (F). All experiments were performed at least three times and error bars
544 represent standard error between all experiments. Error bars are omitted if smaller than the data marker, and
545 p-values were generated using one-way ANOVA.
546 **Fig 3. Production of cell-free and cell-associated HCMV progeny virus in fibroblasts.** Replicate cultures
547 of fibroblasts were infected at MOI 1 with TB, TR, or ME. At 7 days post infection, the number of infected cells
548 in each culture was determined by flow cytometry for GFP expression, and the cumulative number of HCMV
549 genomes in each culture was determined by qPCR; (A) culture supernatants, (C) cell-associated genomes.
550 Specific infectivity was determined by titration on fibroblasts cultures and expressed as the ratio of genomes
551 per infectious unit (IU); (B) cell-free, (D) cell-associated. Error bars represent the standard error of three
552 separate experiments, and p-values were generated using one-way ANOVA.
553 **Fig 4. Production of cell-free and cell-associated HCMV progeny virus in epithelial cells.** Replicate
554 cultures of epithelial cells were infected with TB, TR or ME. At 7 days post infection, the number of infected
555 cells in each culture was determined by flow cytometry for GFP expression, and the cumulative number of
556 HCMV genomes in each culture was determined by qPCR; (A) culture supernatants, (C) cell-associated
557 genomes. Specific infectivity was determined by titration on epithelial cells and expressed as the ratio of
558 genomes per infectious unit (IU); (B) cell-free, (D) cell-associated. Error bars represent the standard error of
559 three separate experiments, and p-values were generated using one-way ANOVA.
560 **Fig 5. Effects of neutralizing antibodies on spread of HCMV strains in fibroblasts and epithelial cells.**
561 Confluent 6cm monolayers of fibroblasts or epithelial cells were infected with 1000 IUs GFP-expressing

562 HCMV strains TB, TR, or ME and allowed to spread in the presence of either anti-gH mAb 14-4b, anti-
563 UL130/131 rabbit sera, or ganciclovir. The average spread rates over 12 days (LN GFP+ cells per day; as in
564 Fig 2) for TB, TR, and ME on fibroblasts (A-C) and epithelial cells (D-F) are shown. Conditions where no
565 spread was detected are designated "n.d.". All experiments were performed three times and error bars
566 represent standard error. P-values were generated by unpaired t-test vs. mock (*<0.05, **<0.01, ***<0.001,
567 ****<0.0001).
568 **Fig 6. Repression of gH/gL/UL128-131 expression by HCMV ME in fibroblasts and epithelial cells**. (A)
569 Tetracycline-repressor protein (tetR) expressing fibroblasts (HFFFtet) or epithelial cells (ARPEtet) or control
570 fibroblasts and epithelial cells were transfected with TetO-firefly luciferase reporter and the relative luciferase
571 activity was measured. (B) Non-reducing SDS-PAGE analysis of ME virions derived from HFFFtet or ARPEtet
572 or control cells. (C) Specific infectivity of virions released from HFFFtet or ARPEtet or control cells.
573 **Fig 7. Effect of gH/gL/UL128-131 repression on spread of HCMV strain ME.** Spread rates (LN GFP+
574 cells per day; as in Fig 2) for HCMV strain ME on tetR-expressing or control fibroblasts (A) or epithelial cells
575 (B) in the presence or absence of neutralizing antibodies. All experiments were performed three times and
576 error bars represent standard error. P-values were generated by unpaired t-test comparing to control cells
577 (*<0.05, **<0.01).
578 **Fig 8. Replication and spread of HCMV strains TB, TR, and ME in RL13-expressing fibroblasts and**
579 **epithelial cells.** (A,E) Spread rates in RL13+ fibroblasts or epithelial cells were determined as in Fig 2 and
580 expressed as relative to the same analyses performed in control cells. (B,F) Spread rates in the presence of
581 neutralizing antibodies were determined as in Fig 5 and expressed as percent inhibition in RL13 fibroblasts or
582 epithelial cells, relative to the same analyses performed in control cells. (C,G, and D,H) Quantity and
583 infectivity (genomes/IU) of cell-associated (CA) and cell-free (CF) progeny virus produced by RL13 expressing
584 fibroblasts or epithelial cells were determined as in Figs 3-4 and expressed as relative to the same analyses
585 performed in control cells. All experiments were performed three times and error bars represent standard
586 error. P-values were generated by unpaired t-test to RL13(-) cells (*<0.05, **<0.01, ***<0.001, ****<0.0001).
587 **Fig 9. Effect of RL13 expression on levels of gH/gL complexes and gB in ME virions.** Equal amounts of
588 ME virions derived from RL13-expressing or control fibroblasts or epithelial cells were separated by SDS-

589 PAGE under non-reducing (A) or reducing (B and C) conditions and analyzed by immunoblot with antibodies
590 directed against gL (A), gB, or major capsid protein (C).

591 **Figure 10. Model of cell-free and cell-associated modes of spread by HCMV.** 1. Progeny virions
592 assemble into compartments derived from the *trans*-Golgi network. 2. Trafficking and release of progeny
593 directed towards apical cell surfaces (2a) or cell junctions (2b). 3. Apically released, cell-free virus diffuses in
594 the extracellular fluid and attaches to an adjacent or a distant cell (3a), whereas virus released to the cell
595 junctions is immediately in contact with the adjacent cell (3b). 4. Entry into the next cell by either the cell-free
596 (4a) or the cell-associated (4b) route may be mediated by either direct fusion between the virion envelope and
597 plasma membrane, or by fusion from within an endosome. 5. Alternatively, some studies have suggested that
598 subviral components may be transferred directly to adjacent cells through transient pores or other intercellular
599 connection mechanisms, such as tunneling nanaotubes (45, 76, 77). Overall, specific infectivity of virions
600 might have a dramatic effect on the efficiency of the cell-free route (2a-4a) where the virus is subject to
601 physical limitations related to diffusion and to inactivation by neutralizing antibodies, complement components,
602 and other host defenses. In contrast, the efficiency of cell-associated routes (2b-4b, and 5) might be more
603 influenced by mechanisms of directed trafficking and intercellular connectivity.

604 **Fig S1. Antibody neutralization of cell-free HCMV.** Equal numbers of fibroblast-derived (A and B) or
605 epithelial-derived (C and D) HCMV TB, TR, or ME were incubated with multiple concentrations of anti-gH mAb
606 14-4b (A and C) or anti-UL130/131 rabbit sera (B and D) for 1hr at RT. Remaining infectivity was determined
607 by titration on either fibroblast (A and B) or epithelial cell (C and D) cultures, and plotted as percent of no
608 antibody control. All experiments were performed in triplicate and error bars represent standard error.

609 **Fig S2. RL13-expressing fibroblasts and epithelial cell lines.** RL13-expressing or control fibroblasts or
610 epithelial cells were analyzed by immunoblot analysis (A), and the relative expression levels were determined
611 by flow cytometry (B). In both analyses, anti-His antibodies were used to detect the His tag on the transduced
612 RL13.

613 **REFERENCES**

614 1. Cui X, Cao Z, Wang S et al. Immunization of Rabbits with Recombinant Human Cytomegalovirus
615 Trimeric versus Monomeric gH/gL Protein Elicits Markedly Higher Titers of Antibody and Neutralization
616 Activity. Int J Mol Sci. 2019;20
617 2. Razonable RR. Drug-resistant cytomegalovirus: clinical implications of specific mutations. Curr Opin
618 Organ Transplant. 2018;23:388-394.
619 3. Cudini J, Roy S, Houldcroft CJ et al. Human cytomegalovirus haplotype reconstruction reveals high
620 diversity due to superinfection and evidence of within-host recombination. Proc Natl Acad Sci U S A.
621 2019;116:5693-5698.
622 4. Lassalle F, Depledge DP, Reeves MB et al. Islands of linkage in an ocean of pervasive recombination
623 reveals two-speed evolution of human cytomegalovirus genomes. Virus Evol. 2016;2:vew017.
624 5. Renzette N, Bhattacharjee B, Jensen JD, Gibson L, Kowalik TF. Extensive genome-wide variability of
625 human cytomegalovirus in congenitally infected infants. PLoS Pathog. 2011;7:e1001344.
626 6. Renzette N, Gibson L, Bhattacharjee B et al. Rapid Intrahost Evolution of Human Cytomegalovirus Is
627 Shaped by Demography and Positive Selection. PLoS Genet. 2013;9:e1003735.
628 7. Sijmons S, Thys K, Mbong Ngwese M et al. High-throughput analysis of human cytomegalovirus
629 genome diversity highlights the widespread occurrence of gene-disrupting mutations and pervasive
630 recombination. J Virol. 2015;89:7673-7695.
631 8. Suárez NM, Wilkie GS, Hage E et al. Human Cytomegalovirus Genomes Sequenced Directly from
632 Clinical Material: Variation, Multiple-Strain Infection, Recombination and Gene Loss. J Infect Dis. 2019
633 9. Suárez NM, Musonda KG, Escriva E et al. Multiple-Strain Infections of Human Cytomegalovirus with
634 High Genomic Diversity are Common In Breast Milk from HIV-Positive Women in Zambia. J Infect Dis.
635 2019
636 10. Dolan A, Cunningham C, Hector RD et al. Genetic content of wild-type human cytomegalovirus. J Gen
637 Virol. 2004;85:1301-1312.
638 11. Stern-Ginossar N, Weisburd B, Michalski A et al. Decoding human cytomegalovirus. Science.
639 2012;338:1088-1093.
640 12. Connolly SA, Jackson JO, Jardetzky TS, Longnecker R. Fusing structure and function: a structural view
641 of the herpesvirus entry machinery. Nat Rev Microbiol. 2011;9:369-381.
642 13. Huber MT, Compton T. Characterization of a novel third member of the human cytomegalovirus
643 glycoprotein H-glycoprotein L complex. J Virol. 1997;71:5391-5398.
644 14. Li L, Nelson JA, Britt WJ. Glycoprotein H-related complexes of human cytomegalovirus: identification of
645 a third protein in the gCIII complex. J Virol. 1997;71:3090-3097.
646 15. Adler B, Scrivano L, Ruzcics Z, Rupp B, Sinzger C, Koszinowski U. Role of human cytomegalovirus
647 UL131A in cell type-specific virus entry and release. J Gen Virol. 2006;87:2451-2460.
648 16. Hahn G, Revello MG, Patrone M et al. Human cytomegalovirus UL131-128 genes are indispensable for
649 virus growth in endothelial cells and virus transfer to leukocytes. J Virol. 2004;78:10023-10033.
650 17. Ryckman BJ, Rainish BL, Chase MC et al. Characterization of the human cytomegalovirus
651 gH/gL/UL128-131 complex that mediates entry into epithelial and endothelial cells. J Virol. 2008;82:60-
652 70.
653 18. Wang D, Shenk T. Human cytomegalovirus UL131 open reading frame is required for epithelial cell
654 tropism. J Virol. 2005;79:10330-10338.
655 19. Vanarsdall AL, Howard PW, Wisner TW, Johnson DC. Human Cytomegalovirus gH/gL Forms a Stable
656 Complex with the Fusion Protein gB in Virions. PLoS Pathog. 2016;12:e1005564.
657 20. Vanarsdall AL, Ryckman BJ, Chase MC, Johnson DC. Human cytomegalovirus glycoproteins gB and
658 gH/gL mediate epithelial cell-cell fusion when expressed either in cis or in trans. J Virol. 2008;82:11837-
659 11850.
660 21. E X, Meraner P, Lu P et al. OR14I1 is a receptor for the human cytomegalovirus pentameric complex
661 and defines viral epithelial cell tropism. Proc Natl Acad Sci U S A. 2019
662 22. Kabanova A, Marcandalli J, Zhou T et al. Platelet-derived growth factor-α receptor is the cellular receptor
663 for human cytomegalovirus gHgLgO trimer. Nat Microbiol. 2016;2016
664 23. Martinez-Martin N, Marcandalli J, Huang CS et al. An Unbiased Screen for Human Cytomegalovirus
665 Identifies Neuropilin-2 as a Central Viral Receptor. Cell. 2018
666 24. Laib Sampaio K, Stegmann C, Brizic I, Adler B, Stanton RJ, Sinzger C. The contribution of pUL74 to
667 growth of human cytomegalovirus is masked in the presence of RL13 and UL128 expression. J Gen

668 Virol. 2016
669 25. Stegmann C, Hochdorfer D, Lieber D et al. A derivative of platelet-derived growth factor receptor alpha
670 binds to the trimer of human cytomegalovirus and inhibits entry into fibroblasts and endothelial cells.
671 PLoS Pathog. 2017;13:e1006273.
672 26. Wille PT, Knoche AJ, Nelson JA, Jarvis MA, Johnson DC. A human cytomegalovirus gO-null mutant fails
673 to incorporate gH/gL into the virion envelope and is unable to enter fibroblasts and epithelial and
674 endothelial cells. J Virol. 2010;84:2585-2596.
675 27. Zhou M, Lanchy JM, Ryckman BJ. Human cytomegalovirus gH/gL/gO promotes the fusion step of entry
676 into all cell types whereas gH/gL/UL128-131 broadens virus tropism through a distinct mechanism. J
677 Virol. 2015
678 28. Liu J, Jardetzky TS, Chin AL, Johnson DC, Vanarsdall AL. The human cytomegalovirus trimer and
679 pentamer promote sequential steps in entry into epithelial and endothelial cells at cell surfaces and
680 endosomes. J Virol. 2018
681 29. Luo MH, Schwartz PH, Fortunato EA. Neonatal neural progenitor cells and their neuronal and glial cell
682 derivatives are fully permissive for human cytomegalovirus infection. J Virol. 2008;82:9994-10007.
683 30. Nogalski MT, Chan GC, Stevenson EV, Collins-McMillen DK, Yurochko AD. The HCMV gH/gL/UL128-
684 131 Complex Triggers the Specific Cellular Activation Required for Efficient Viral Internalization into
685 Target Monocytes. PLoS Pathog. 2013;9:e1003463.
686 31. Ryckman BJ, Jarvis MA, Drummond DD, Nelson JA, Johnson DC. Human cytomegalovirus entry into
687 epithelial and endothelial cells depends on genes UL128 to UL150 and occurs by endocytosis and low-
688 pH fusion. J Virol. 2006;80:710-722.
689 32. Auerbach M, Yan D, Fouts A et al. Characterization of the guinea pig CMV gH/gL/GP129/GP131/GP133
690 complex in infection and spread. Virology. 2013;441:75-84.
691 33. Coleman S, Hornig J, Maddux S, Choi KY, McGregor A. Viral Glycoprotein Complex Formation,
692 Essential Function and Immunogenicity in the Guinea Pig Model for Cytomegalovirus. PLoS One.
693 2015;10:e0135567.
694 34. Lemmermann NA, Krmpotic A, Podlech J et al. Non-redundant and Redundant Roles of
695 Cytomegalovirus gH/gL Complexes in Host Organ Entry and Intra-tissue Spread. PLoS Pathog.
696 2015;11:e1004640.
697 35. Scrivano L, Sinzger C, Nitschko H, Koszinowski UH, Adler B. HCMV spread and cell tropism are
698 determined by distinct virus populations. PLoS Pathog. 2011;7:e1001256.
699 36. Wagner FM, Brizic I, Prager A et al. The Viral Chemokine MCK-2 of Murine Cytomegalovirus Promotes
700 Infection as Part of a gH/gL/MCK-2 Complex. PLoS Pathog. 2013;9:e1003493.
701 37. Yunis J, Farrell HE, Bruce K et al. Murine Cytomegalovirus glycoprotein O promotes epithelial cell
702 infection. J Virol. 2018
703 38. Murrell I, Tomasec P, Wilkie GS, Dargan DJ, Davison AJ, Stanton RJ. Impact of sequence variation in
704 the UL128 locus on production of human cytomegalovirus in fibroblast and epithelial cells. J Virol.
705 2013;87:10489-10500.
706 39. Zhang L, Zhou M, Stanton R, Kamil J, Ryckman BJ. Expression levels of glycoprotein O (gO) vary
707 between strains of human cytomegalovirus, influencing the assembly of gH/gL complexes and virion
708 infectivity. J Virol. 2018
709 40. Stanton RJ, Baluchova K, Dargan DJ et al. Reconstruction of the complete human cytomegalovirus
710 genome in a BAC reveals RL13 to be a potent inhibitor of replication. J Clin Invest. 2010;120:3191-3208.
711 41. Sinzger C, Hahn G, Digel M et al. Cloning and sequencing of a highly productive, endotheliotropic virus
712 strain derived from human cytomegalovirus TB40/E. J Gen Virol. 2008;89:359-368.
713 42. Murrell I, Bedford C, Ladell K et al. The pentameric complex drives immunologically covert cell-cell
714 transmission of wild-type human cytomegalovirus. Proc Natl Acad Sci U S A. 2017
715 43. Wu K, Oberstein A, Wang W, Shenk T. Role of PDGF receptor-α during human cytomegalovirus entry
716 into fibroblasts. Proc Natl Acad Sci U S A. 2018
717 44. Wu Y, Prager A, Boos S et al. Human cytomegalovirus glycoprotein complex gH/gL/gO uses PDGFR-α
718 as a key for entry. PLoS Pathog. 2017;13:e1006281.
719 45. Digel M, Sampaio KL, Jahn G, Sinzger C. Evidence for direct transfer of cytoplasmic material from
720 infected to uninfected cells during cell-associated spread of human cytomegalovirus. J Clin Virol.
721 2006;37:10-20.
722 46. Gerna G, Percivalle E, Baldanti F et al. Human cytomegalovirus replicates abortively in
723 polymorphonuclear leukocytes after transfer from infected endothelial cells via transient microfusion

events. J Virol. 2000;74:5629-5638.
47. Silva MC, Schroer J, Shenk T. Human cytomegalovirus cell-to-cell spread in the absence of an essential assembly protein. Proc Natl Acad Sci U S A. 2005;102:2081-2086.
48. Cui X, Freed DC, Wang D et al. Impact of antibodies and strain polymorphisms on cytomegalovirus entry and spread in fibroblasts and epithelial cells. J Virol. 2017
49. Gerna G, Percivalle E, Perez L, Lanzavecchia A, Lilleri D. Monoclonal antibodies to different components of the human cytomegalovirus (HCMV) pentamer gH/gL/pUL128L and trimer gH/gL/gO as well as antibodies elicited during primary HCMV infection prevent epithelial cell syncytium formation. J Virol. 2016
50. Zhou M, Yu Q, Wechsler A, Ryckman BJ. Comparative analysis of gO isoforms reveals that strains of human cytomegalovirus differ in the ratio of gH/gL/gO and gH/gL/UL128-131 in the virion envelope. J Virol. 2013;87:9680-9690.
51. Bogner E, Reschke M, Reis B, Reis E, Britt W, Radsak K. Recognition of compartmentalized intracellular analogs of glycoprotein H of human cytomegalovirus. Arch Virol. 1992;126:67-80.
52. Schultz EP, Lanchy JM, Ellerbeck EE, Ryckman BJ. Scanning mutagenesis of human cytomegalovirus gH/gL. J Virol. 2015
53. Baldanti F, Underwood MR, Talarico CL et al. The Cys607-->Tyr change in the UL97 phosphotransferase confers ganciclovir resistance to two human cytomegalovirus strains recovered from two immunocompromised patients. Antimicrob Agents Chemother. 1998;42:444-446.
54. Dargan DJ, Douglas E, Cunningham C et al. Sequential mutations associated with adaptation of human cytomegalovirus to growth in cell culture. J Gen Virol. 2010;91:1535-1546.
55. Murrell I, Wilkie GS, Davison AJ et al. Genetic Stability of Bacterial Artificial Chromosome-Derived Human Cytomegalovirus during Culture In Vitro. J Virol. 2016;90:3929-3943.
56. Britt WJ, Vugler LG. Processing of the gp55-116 envelope glycoprotein complex (gB) of human cytomegalovirus. J Virol. 1989;63:403-410.
57. Schoppel K, Hassfurther E, Britt W, Ohlin M, Borrebaeck CA, Mach M. Antibodies specific for the antigenic domain 1 of glycoprotein B (gpUL55) of human cytomegalovirus bind to different substructures. Virology. 1996;216:133-145.
58. Spaete RR, Saxena A, Scott PI et al. Sequence requirements for proteolytic processing of glycoprotein B of human cytomegalovirus strain Towne. J Virol. 1990;64:2922-2931.
59. Sinzger C, Schmidt K, Knapp J et al. Modification of human cytomegalovirus tropism through propagation in vitro is associated with changes in the viral genome. J Gen Virol. 1999;80:2867-2877.
60. Galitska G, Biolatti M, De Andrea M et al. Biological relevance of Cytomegalovirus genetic variability in congenitally and postnatally infected children. J Clin Virol. 2018;108:132-140.
61. Subramanian N, Wu Z, Mertens TM. Phenotypic characterization of human cytomegalovirus strains in cell cultures based on their transmission kinetics. J Gen Virol. 2016;97:2376-2386.
62. Ourahmane A, Cui X, He L et al. Inclusion of Antibodies to Cell Culture Media Preserves the Integrity of Genes Encoding RL13 and the Pentameric Complex Components During Fibroblast Passage of Human Cytomegalovirus. Viruses. 2019;11
63. Strive T, Borst E, Messerle M, Radsak K. Proteolytic processing of human cytomegalovirus glycoprotein B is dispensable for viral growth in culture. J Virol. 2002;76:1252-1264.
64. Hutt-Fletcher LM. Epstein-Barr virus entry. J Virol. 2007;81:7825-7832.
65. Cannon MJ, Hyde TB, Schmid DS. Review of cytomegalovirus shedding in bodily fluids and relevance to congenital cytomegalovirus infection. Rev Med Virol. 2011;21:240-255.
66. Chou S, Merigan TC. Rapid detection and quantitation of human cytomegalovirus in urine through DNA hybridization. N Engl J Med. 1983;308:921-925.
67. Gerna G, Percivalle E, Sarasini A, Revello MG. Human cytomegalovirus and human umbilical vein endothelial cells: restriction of primary isolation to blood samples and susceptibilities of clinical isolates from other sources to adaptation. J Clin Microbiol. 2002;40:233-238.
68. Kitamura T, Koshino Y, Shibata F et al. Retrovirus-mediated gene transfer and expression cloning: powerful tools in functional genomics. Exp Hematol. 2003;31:1007-1014.
69. Stewart SA, Dykxhoorn DM, Palliser D et al. Lentivirus-delivered stable gene silencing by RNAi in primary cells. RNA. 2003;9:493-501.
70. Sancak Y, Peterson TR, Shaul YD et al. The Rag GTPases bind raptor and mediate amino acid signaling to mTORC1. Science. 2008;320:1496-1501.
71. Dull T, Zufferey R, Kelly M et al. A third-generation lentivirus vector with a conditional packaging system.

780 J Virol. 1998;72:8463-8471.
781 72. Murphy E, Yu D, Grimwood J et al. Coding potential of laboratory and clinical strains of human
782 cytomegalovirus. Proc Natl Acad Sci U S A. 2003;100:14976-14981.
783 73. Tischer BK, Smith GA, Osterrieder N. En passant mutagenesis: a two step markerless red
784 recombination system. Methods Mol Biol. 2010;634:421-430.
785 74. Chee M, Rudolph SA, Plachter B, Barrell B, Jahn G. Identification of the major capsid protein gene of
786 human cytomegalovirus. J Virol. 1989;63:1345-1353.
787 75. Rooney JP, Ryde IT, Sanders LH et al. PCR based determination of mitochondrial DNA copy number in
788 multiple species. Methods Mol Biol. 2015;1241:23-38.
789 76. Gerna G, Percivalle E, Lilleri D et al. Dendritic-cell infection by human cytomegalovirus is restricted to
790 strains carrying functional UL131-128 genes and mediates efficient viral antigen presentation to CD8+ T
791 cells. J Gen Virol. 2005;86:275-284.
792 77. Panasiuk M, Rychłowski M, Derewońko N, Bieńkowska-Szewczyk K. Tunneling Nanotubes as a Novel
793 Route of Cell-to-Cell Spread of Herpesviruses. J Virol. 2018;92
794

795 **Figure 1**
796
797

A. Fibroblasts

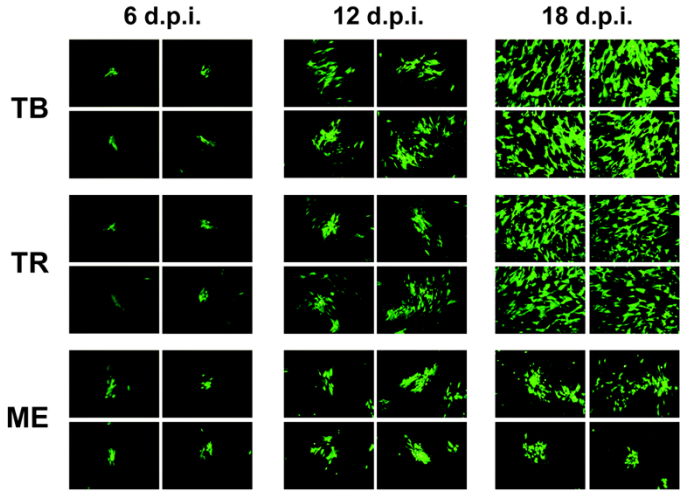

B. Epithelial Cells

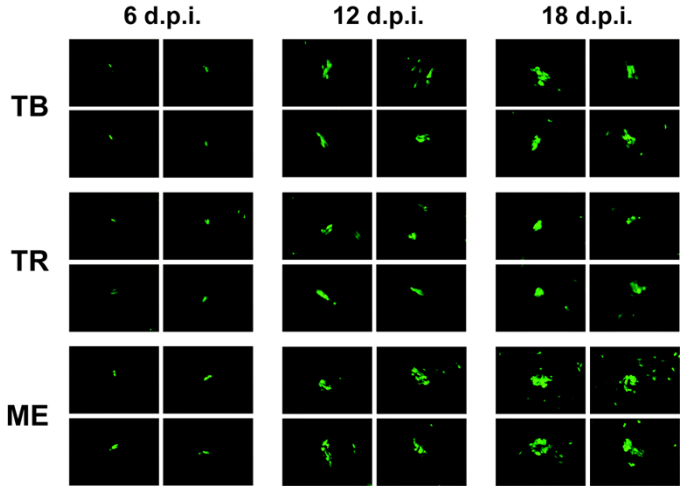

798
799
800
801
802
803 **Fig 1. Comparison of focal spread patterns of distinct HCMV stains.** Confluent monolayers of fibroblasts
804 (A) or epithelial cells (B) were infected at an MOI of 0.001 with GFP-expressing HCMV strains TB, TR, or ME.
805 Foci were documented by fluorescence microscopy at 6, 12, and 18 days post infection. Four representative
806 fields (10X) are shown for each.
807
808
809
810

Figure 2

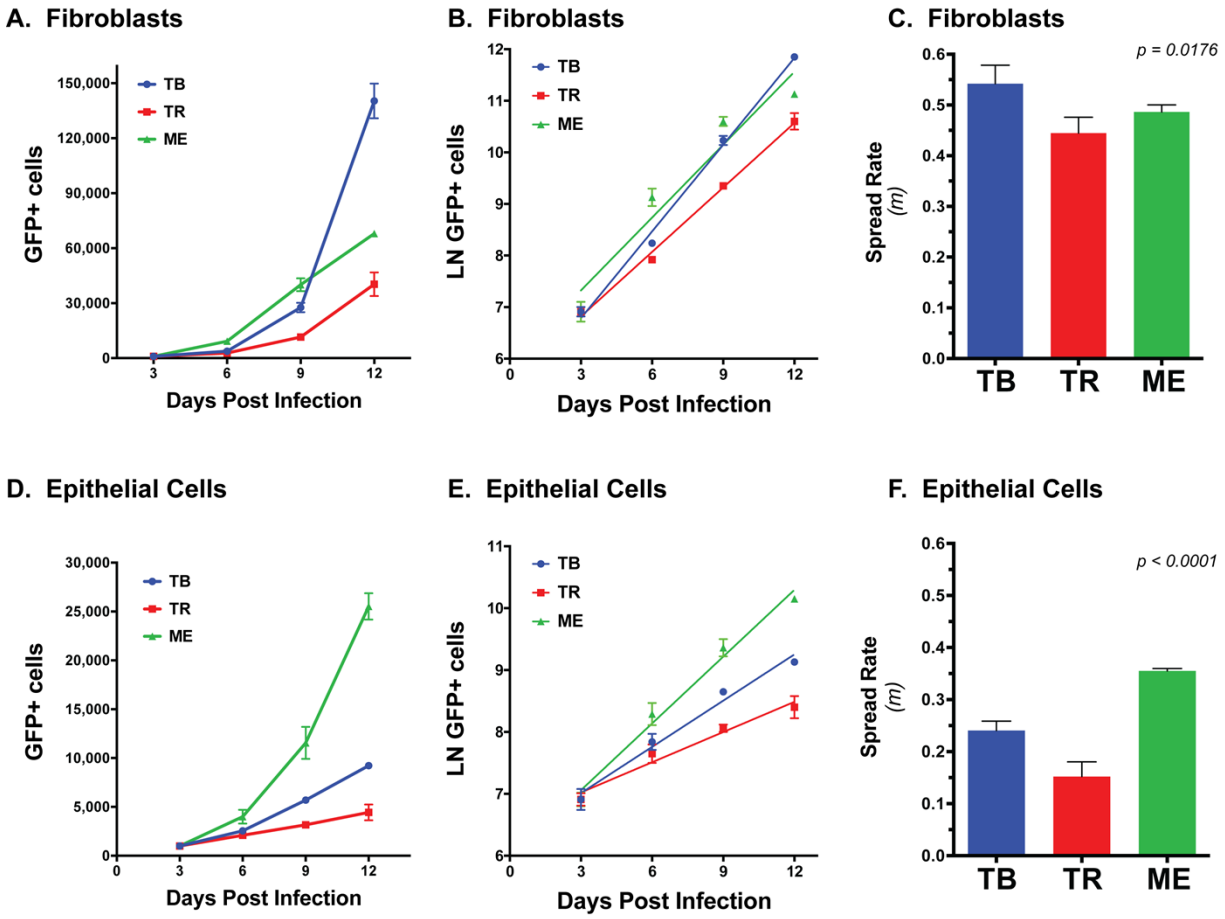

Fig 2. Quantitation of HCMV spread by in fibroblasts and epithelial cells. Confluent 6cm monolayers of fibroblasts (A) or epithelial cells (D) were infected with 1000 IUs of GFP-expressing HCMV strains TB, TR, or ME. The number of infected cells at 3, 6, 9, and 12 days post infection was determined by flow cytometry. To determine exponential growth rates, the LN GFP+ cells is plotted at each time point for fibroblasts (B) and epithelial cells (E). The average spread rates (LN GFP+ cells per day) of the three strains were determined for fibroblasts (C) and epithelial cells (F). All experiments were performed at least three times and error bars represent standard error between all experiments. Error bars are omitted if smaller than the data marker, and p-values were generated using one-way ANOVA.

835 **Figure 3**
836
837

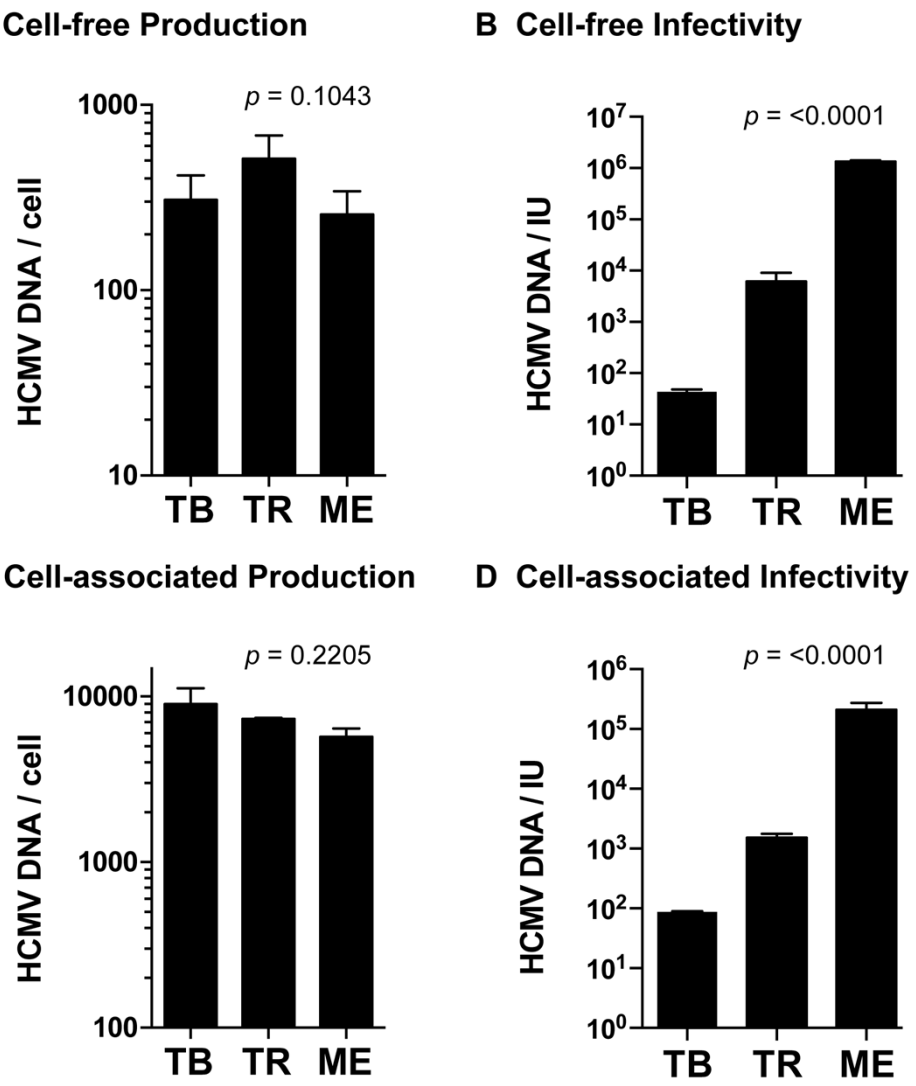

838
839
840
841
842
843 **Fig 3. Production of cell-free and cell-associated HCMV progeny virus in fibroblasts.** Replicate cultures
844 of fibroblasts were infected at MOI 1 with TB, TR, or ME. At 7 days post infection, the number of infected cells
845 in each culture was determined by flow cytometry for GFP expression, and the cumulative number of HCMV
846 genomes in each culture was determined by qPCR; (A) culture supernatants, (C) cell-associated genomes.
847 Specific infectivity was determined by titration on fibroblasts cultures and expressed as the ratio of genomes
848 per infectious unit (IU); (B) cell-free, (D) cell-associated. Error bars represent the standard error of three
849 separate experiments, and p-values were generated using one-way ANOVA.
850
851
852
853

854 **Figure 4**
855
856

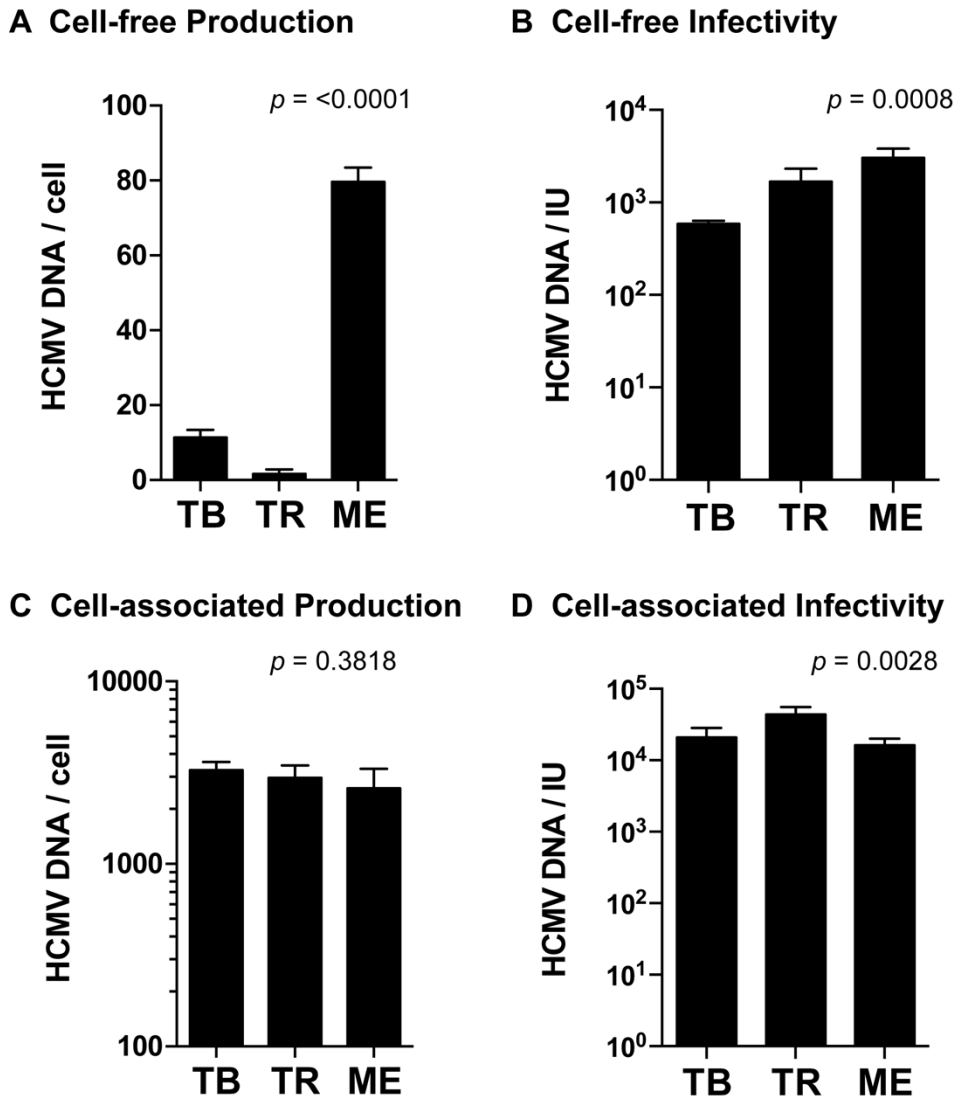

857
858
859
860 **Fig 4. Production of cell-free and cell-associated HCMV progeny virus in epithelial cells.** Replicate
861 cultures of epithelial cells were infected with TB, TR or ME. At 7 days post infection, the number of infected
862 cells in each culture was determined by flow cytometry for GFP expression, and the cumulative number of
863 HCMV genomes in each culture was determined by qPCR; (A) culture supernatants, (C) cell-associated
864 genomes. Specific infectivity was determined by titration on epithelial cells and expressed as the ratio of
865 genomes per infectious unit (IU); (B) cell-free, (D) cell-associated. Error bars represent the standard error of
866 three separate experiments, and p-values were generated using one-way ANOVA.

868 **Figure S1**
869
870
871

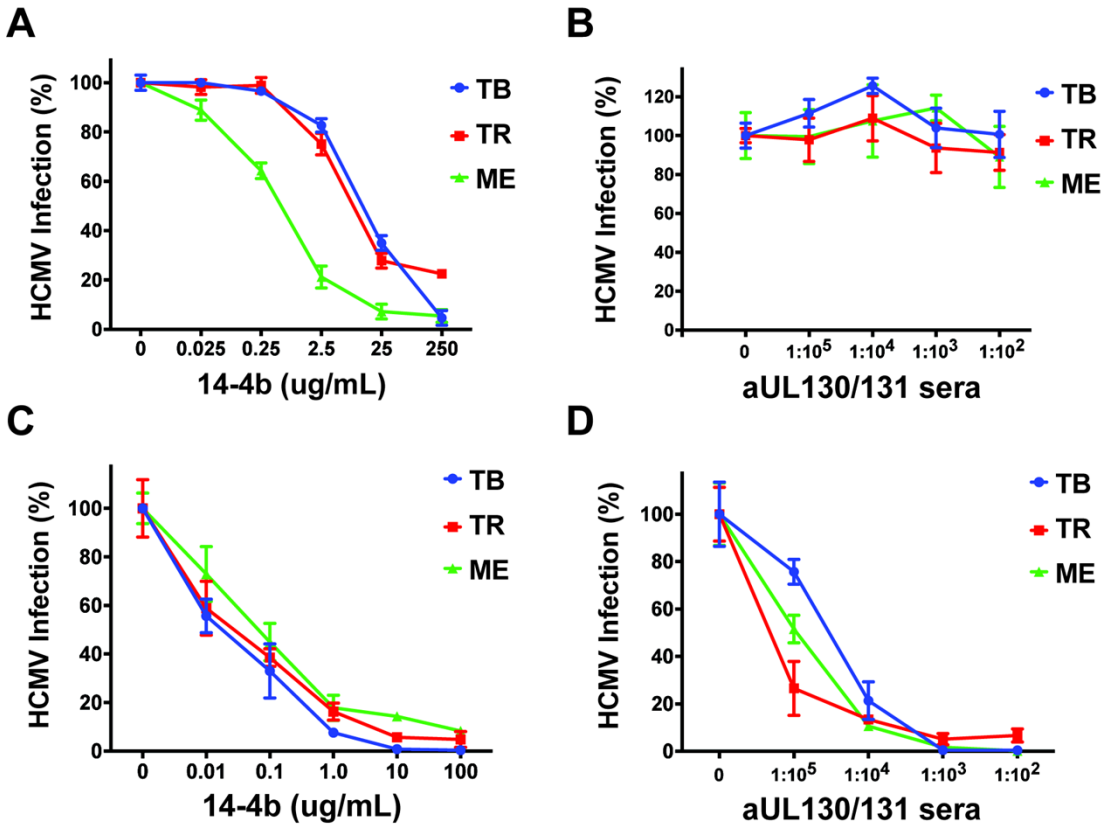

872
873
874
875
876
877 **Fig S1. Antibody neutralization of cell-free HCMV.** Equal numbers of fibroblast-derived (A and B) or
878 epithelial-derived (C and D) HCMV TB, TR, or ME were incubated with multiple concentrations of anti-gH mAb
879 14-4b (A and C) or anti-UL130/131 rabbit sera (B and D) for 1hr at RT. Remaining infectivity was determined
880 by titration on either fibroblast (A and B) or epithelial cell (C and D) cultures, and plotted as percent of no
881 antibody control. All experiments were performed in triplicate and error bars represent standard error.
882
883
884
885
886
887
888
889
890
891

892 **Figure 5**
893

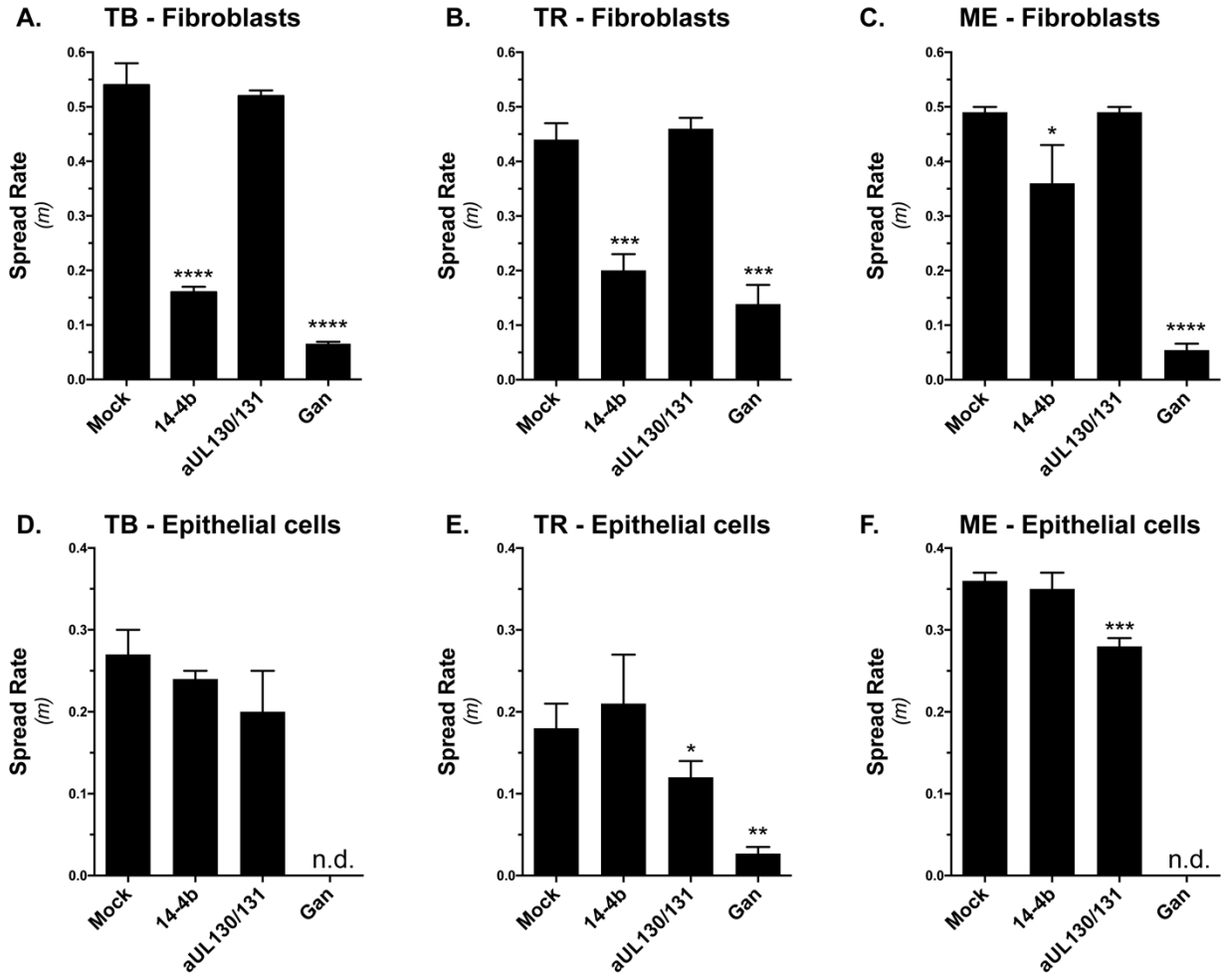

894
895
896
897
898 **Fig 5. Effects of neutralizing antibodies on spread of HCMV strains in fibroblasts and epithelial cells.**
899 Confluent 6cm monolayers of fibroblasts or epithelial cells were infected with 1000 IUs GFP-expressing
900 HCMV strains TB, TR, or ME and allowed to spread in the presence of either anti-gH mAb 14-4b, anti-
901 UL130/131 rabbit sera, or ganciclovir. The average spread rates over 12 days (LN GFP+ cells per day; as in
902 Fig 2) for TB, TR, and ME on fibroblasts (A-C) and epithelial cells (D-F) are shown. Conditions where no
903 spread was detected are designated "n.d.". All experiments were performed three times and error bars
904 represent standard error. P-values were generated by unpaired t-test vs. mock (*<0.05, **<0.01, ***<0.001,
905 ****<0.0001).
906
907
908
909
910
911

912 **Figure 6**
913
914

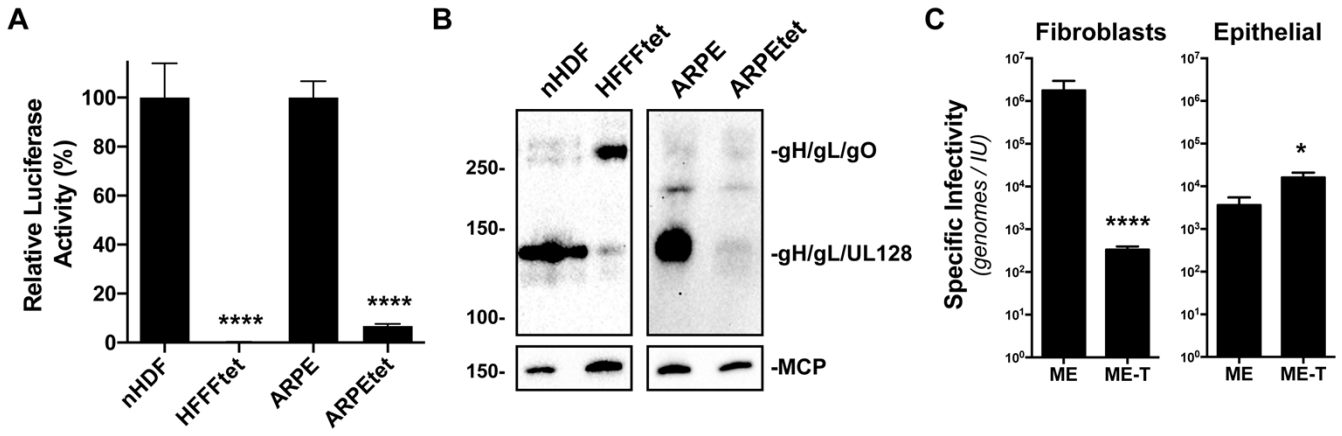

915
916
917 **Fig 6. Repression of gH/gL/UL128-131 expression by HCMV ME in fibroblasts and epithelial cells**. (A)
918 Tetracycline-repressor protein (tetR) expressing fibroblasts (HFFFtet) or epithelial cells (ARPEtet) or control
919 fibroblasts and epithelial cells were transfected with TetO-firefly luciferase reporter and the relative luciferase
920 activity was measured. (B) Non-reducing SDS-PAGE analysis of ME virions derived from HFFFtet or ARPEtet
921 or control cells. (C) Specific infectivity of virions released from HFFFtet or ARPEtet or control cells. P-values
922 were generated by unpaired t-test to tetR(-) cells (*<0.05, **<0.01, ***<0.001, ****<0.0001).
923
924

925 **Figure 7**
926
927

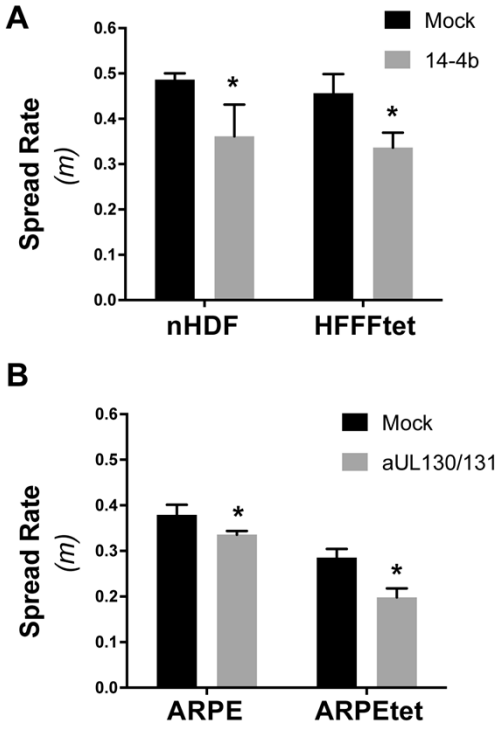

928
929
930
931
932
933 **Fig 7. Effect of gH/gL/UL128-131 repression on spread of HCMV strain ME.** Spread rates (LN GFP+
934 cells per day; as in Fig 2) for HCMV strain ME on tetR-expressing or control fibroblasts (A) or epithelial cells
935 (B) in the presence of absence of neutralizing antibodies. All experiments were performed three times and
936 error bars represent standard error. P-values were generated by unpaired t-test comparing to control cells
937 (*<0.05, **<0.01).
938
939
940
941
942
943
944
945
946
947
948
949
950
951

952 **Figure S2**

953
954
955

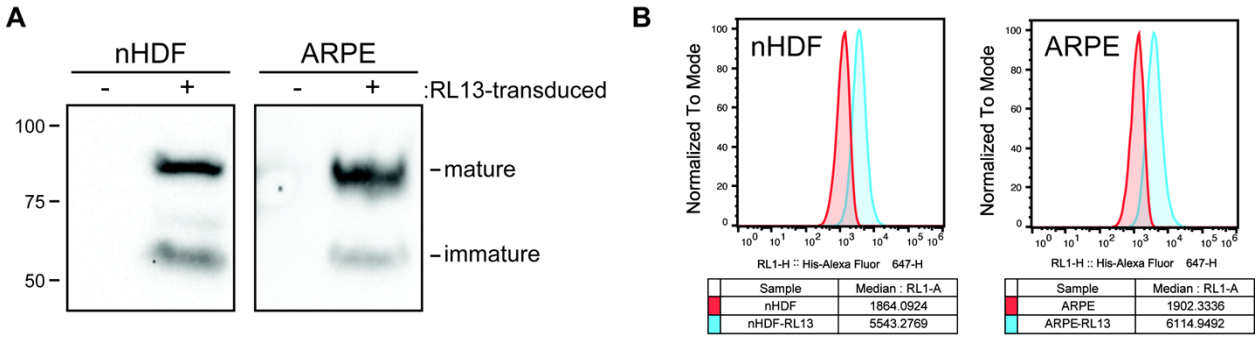

956
957
958

959 **Fig S2. RL13-expressing fibroblasts and epithelial cell lines.** RL13-expressing or control fibroblasts or
960 epithelial cells were analyzed by immunoblot analysis (A), and the relative expression levels were determined
961 by flow cytometry (B). In both analyses, anti-His antibodies were used to detect the His tag on the transduced
962 RL13.

963 **Figure 8**

964

965

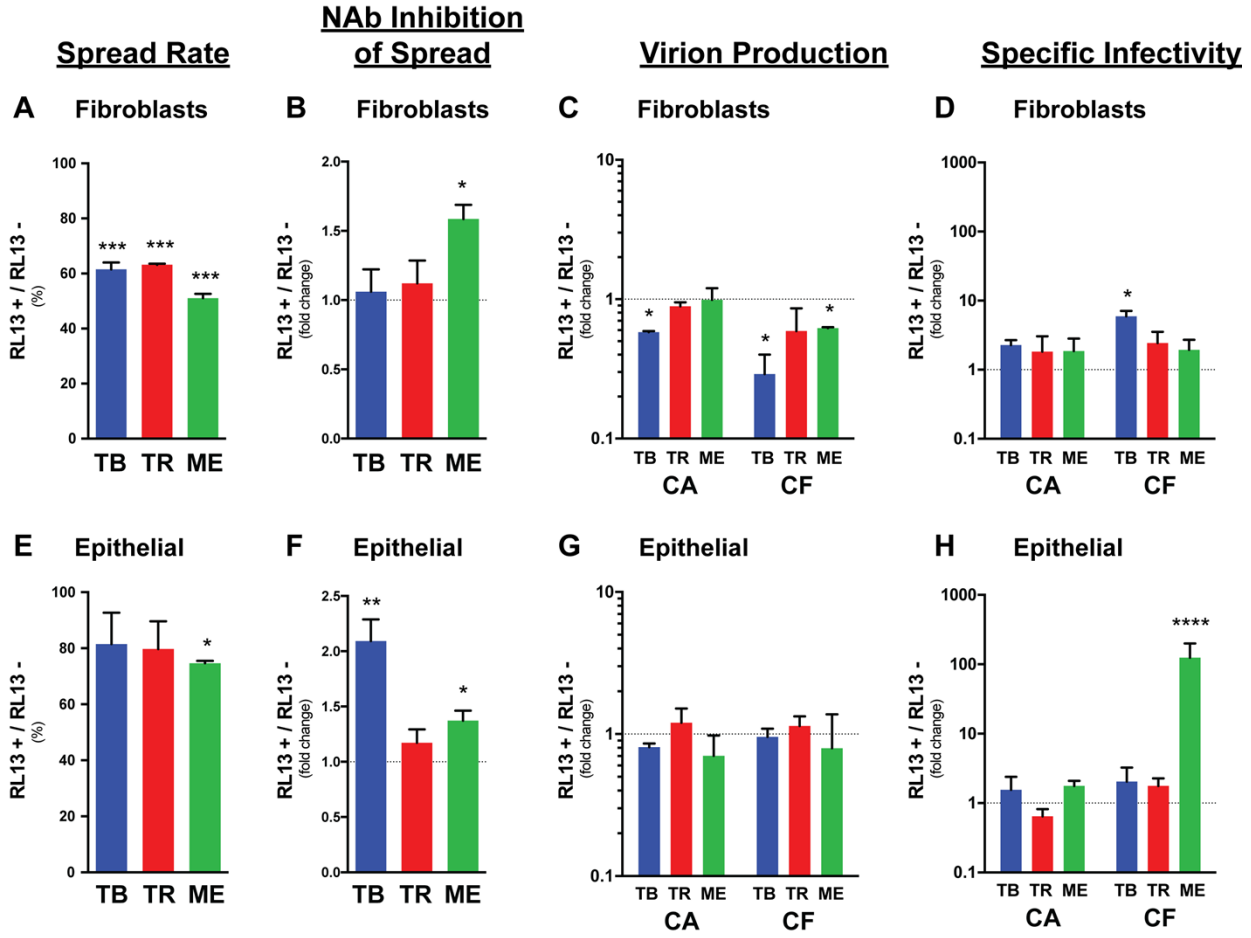

966

967

968 **Fig 8. Replication and spread of HCMV strains TB, TR, and ME in RL13-expressing fibroblasts and**
969 **epithelial cells.** (A,E) Spread rates in RL13+ fibroblasts or epithelial cells were determined as in Fig 2 and
970 expressed as relative to the same analyses performed in control cells. (B,F) Spread rates in the presence of
971 neutralizing antibodies were determined as in Fig 5 and expressed as percent inhibition in RL13 fibroblasts or
972 epithelial cells, relative to the same analyses performed in control cells. (C,G, and D,H) Quantity and
973 infectivity (genomes/IU) of cell-associated (CA) and cell-free (CF) progeny virus produced by RL13 expressing
974 fibroblasts or epithelial cells were determined as in Figs 3-4 and expressed as relative to the same analyses
975 performed in control cells. All experiments were performed three times and error bars represent standard
976 error. P-values were generated by unpaired t-test to RL13(-) cells (*<0.05, **<0.01, ***<0.001, ****<0.0001).

977

978 **Figure 9**
979

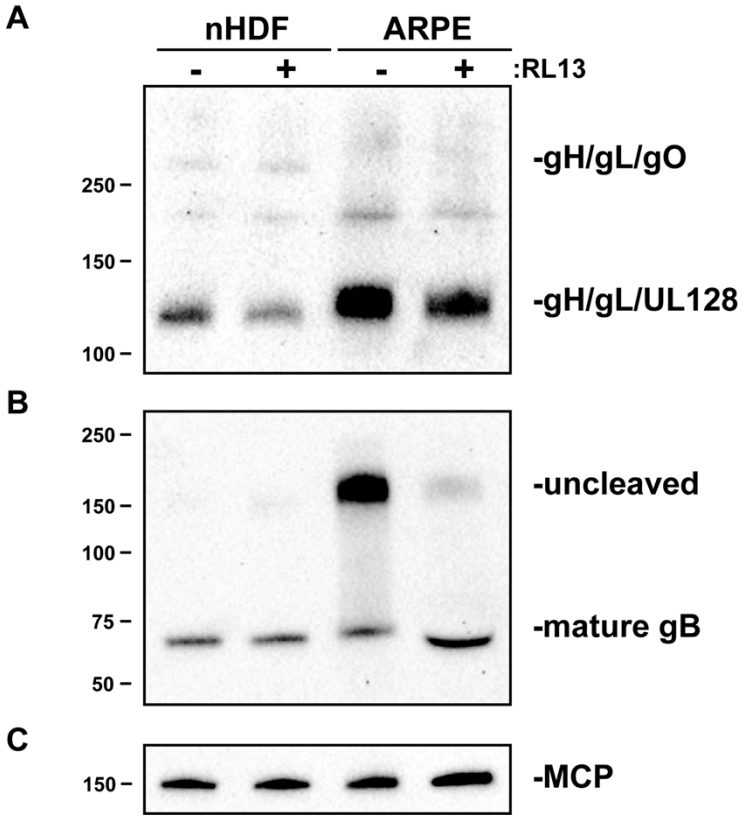

980
981
982
983
984
985 **Fig 9. Effect of RL13 expression on levels of gH/gL complexes and gB in ME virions.** Equal amounts of
986 ME virions derived from RL13-expressing or control fibroblasts or epithelial cells were separated by SDS-
987 PAGE under non-reducing (A) or reducing (B and C) conditions and analyzed by immunoblot with antibodies
988 directed against gL (A), gB, or major capsid protein (C).
989

990 **Figure 10**
991
992

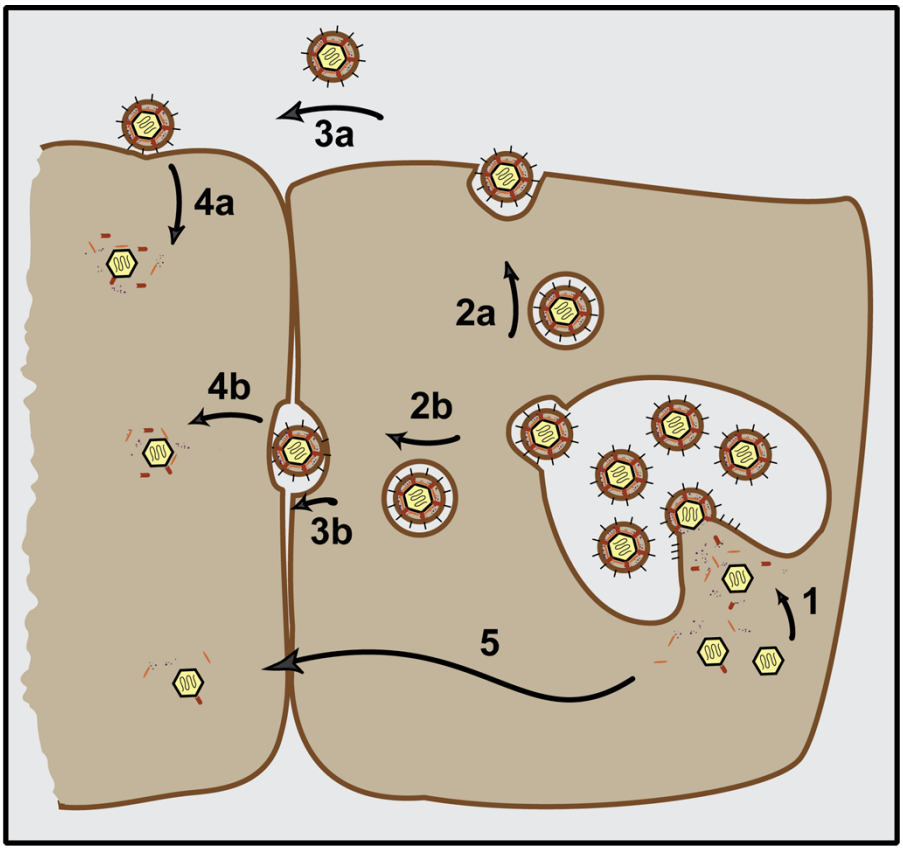

993
994
995 **Figure 10. Model of cell-free and cell-associated modes of spread by HCMV.** 1. Progeny virions
996 assemble into compartments derived from the *trans*-Golgi network. 2. Trafficking and release of progeny
997 directed towards apical cell surfaces (2a) or cell junctions (2b). 3. Apically released, cell-free virus diffuses in
998 the extracellular fluid and attaches to an adjacent or a distant cell (3a), whereas virus released to the cell
999 junctions is immediately in contact with the adjacent cell. 4. Entry into the next cell by either the cell-free (4a)
1000 or the cell-associated (4b) route may be mediated by either direct fusion between the virion envelope and
1001 plasma membrane, or by fusion from within an endosome. 5. Alternatively, some studies have suggested that
1002 subviral components may be transferred directly to adjacent cells through transient pores or other intercellular
1003 connection mechanisms, such as tunneling nanaotubes (45, 76, 77). Overall, specific infectivity of virions
1004 might have a dramatic effect on the efficiency of the cell-free route (2a-4a) where the virus is subject to
1005 physical limitations related to diffusion and to inactivation by neutralizing antibodies, complement components,
1006 and other host defenses. In contrast, the efficiency of cell-associated routes (2b-4b, and 5) might be more
1007 influenced by mechanisms of directed trafficking and intercellular connectivity.

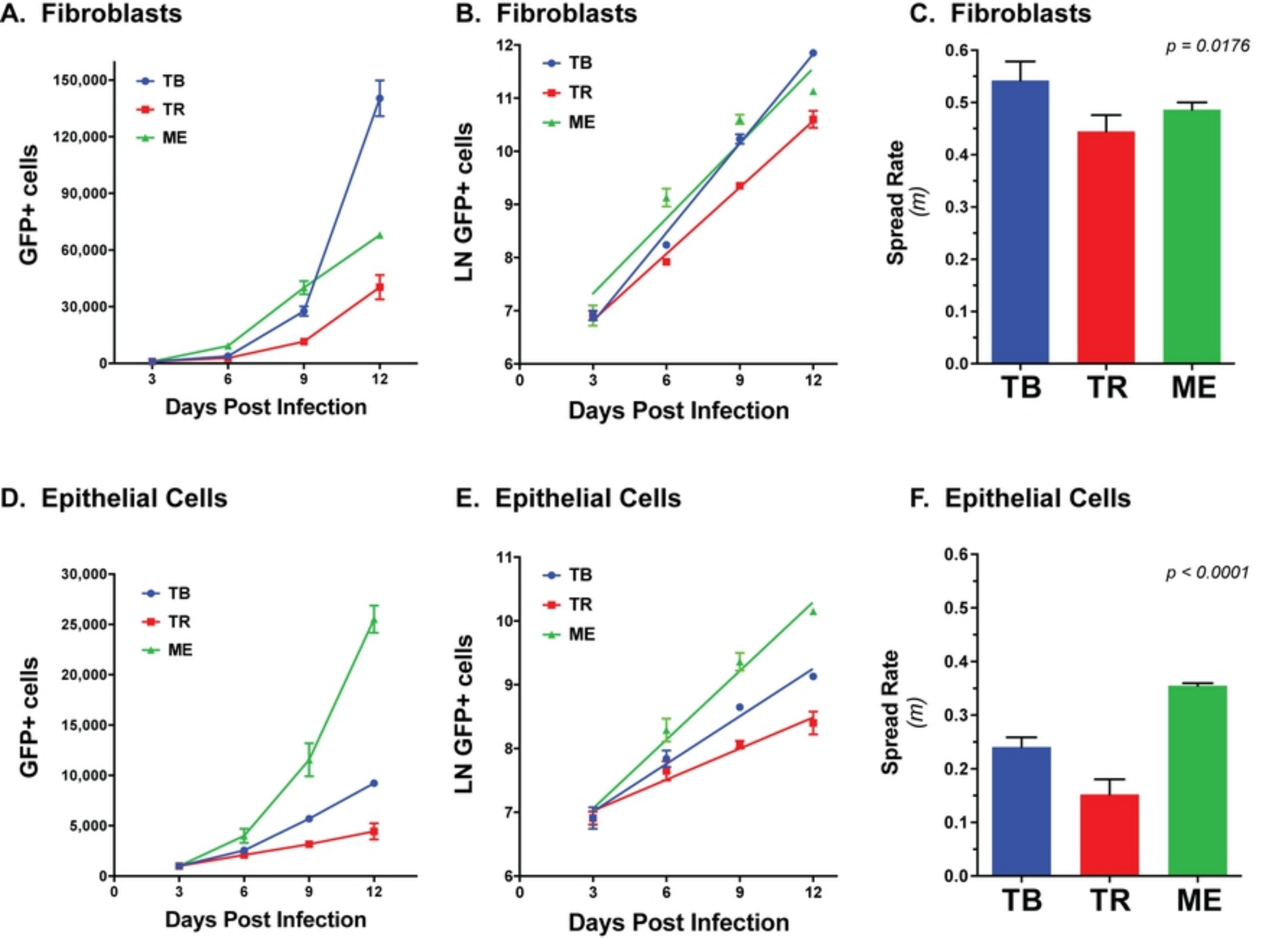
A. Fibroblasts
GFP+ cells
Days Post Infection
TB
TR
ME
B. Fibroblasts
LN GFP+ cells
Days Post Infection
C. Fibroblasts
Spread Rate (m)
p = 0.0176
D. Epithelial Cells
E. Epithelial Cells
F. Epithelial Cells
p < 0.0001

Figure 2

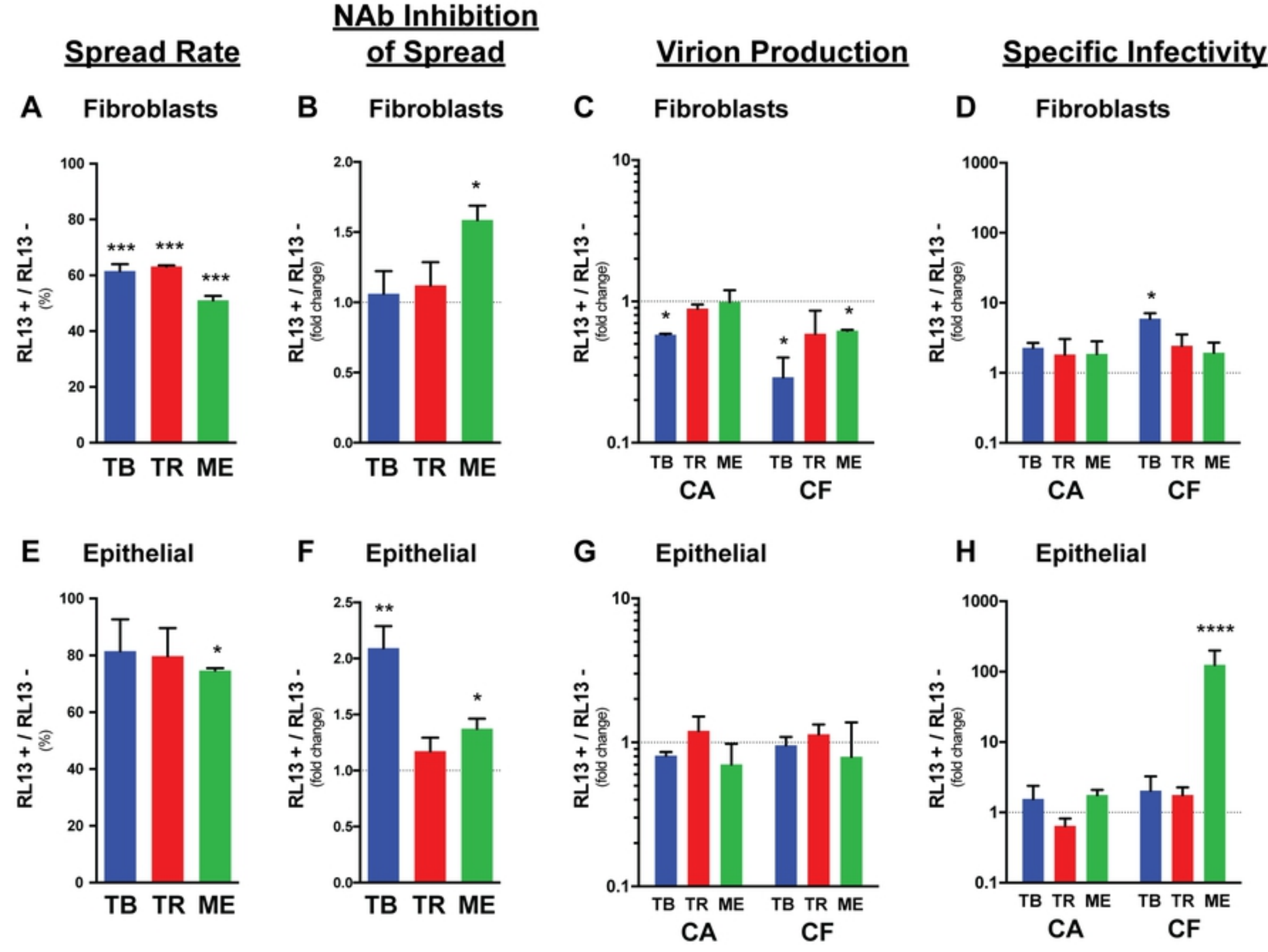
Spread Rate
NAb Inhibition of Spread
Virion Production
Specific Infectivity
A Fibroblasts
B Fibroblasts
C Fibroblasts
D Fibroblasts
E Epithelial
F Epithelial
G Epithelial
H Epithelial
RL13 + / RL13 - (%)
RL13 + / RL13 - (fold change)
TB TR ME
CA CF
***
**
*
****

Figure 8

A. Fibroblasts

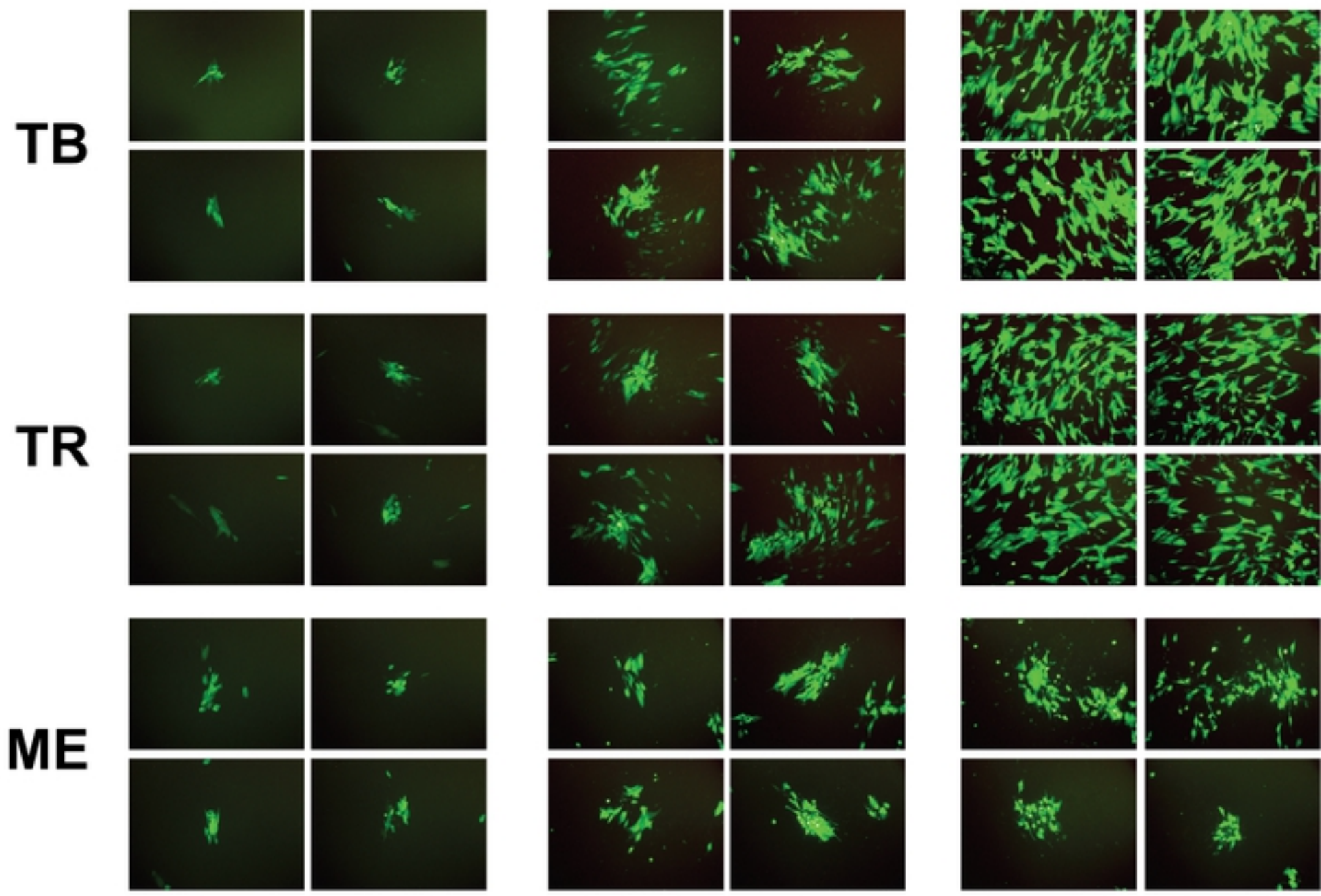

B. Epithelial Cells

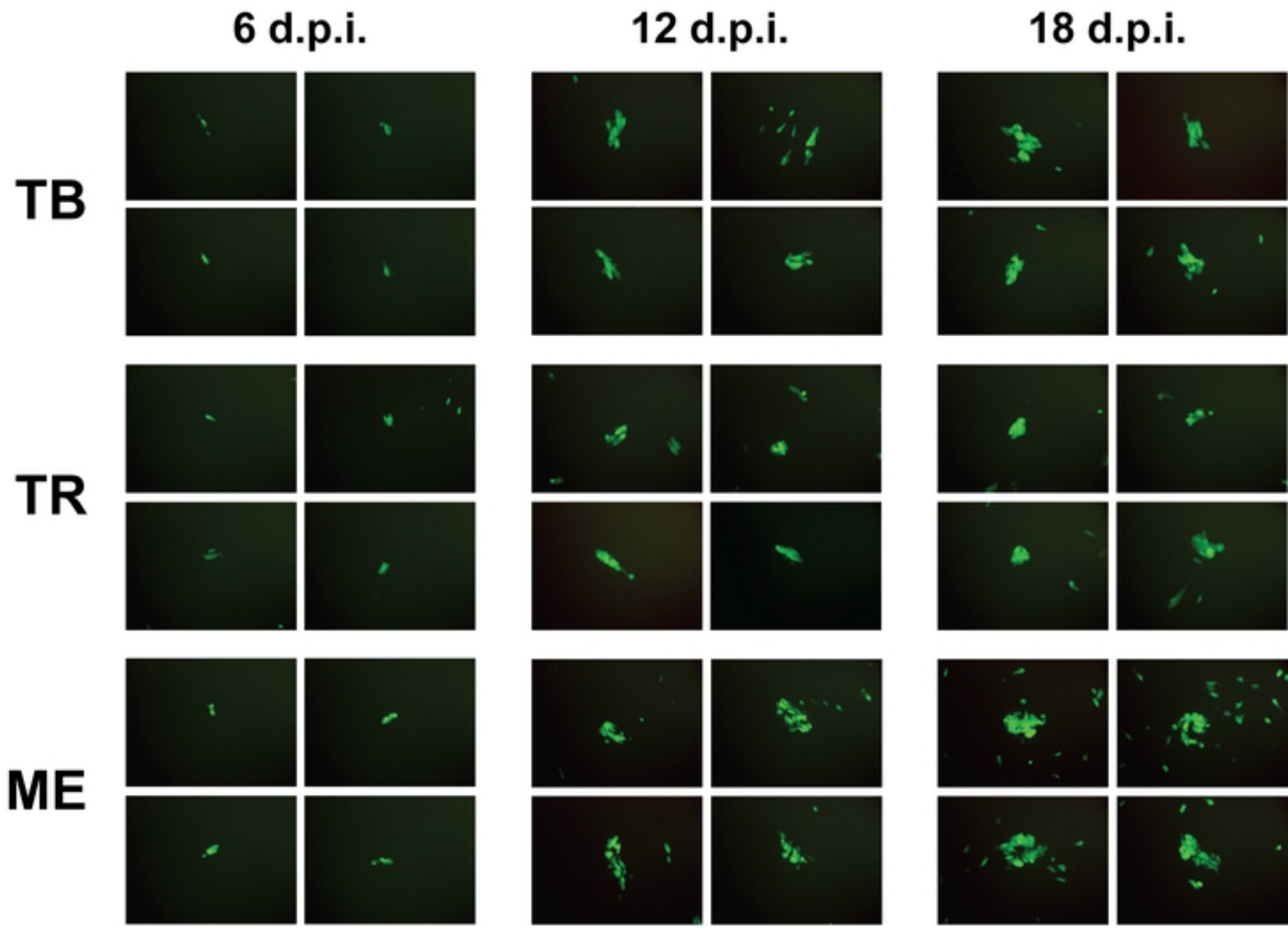

Figure 1

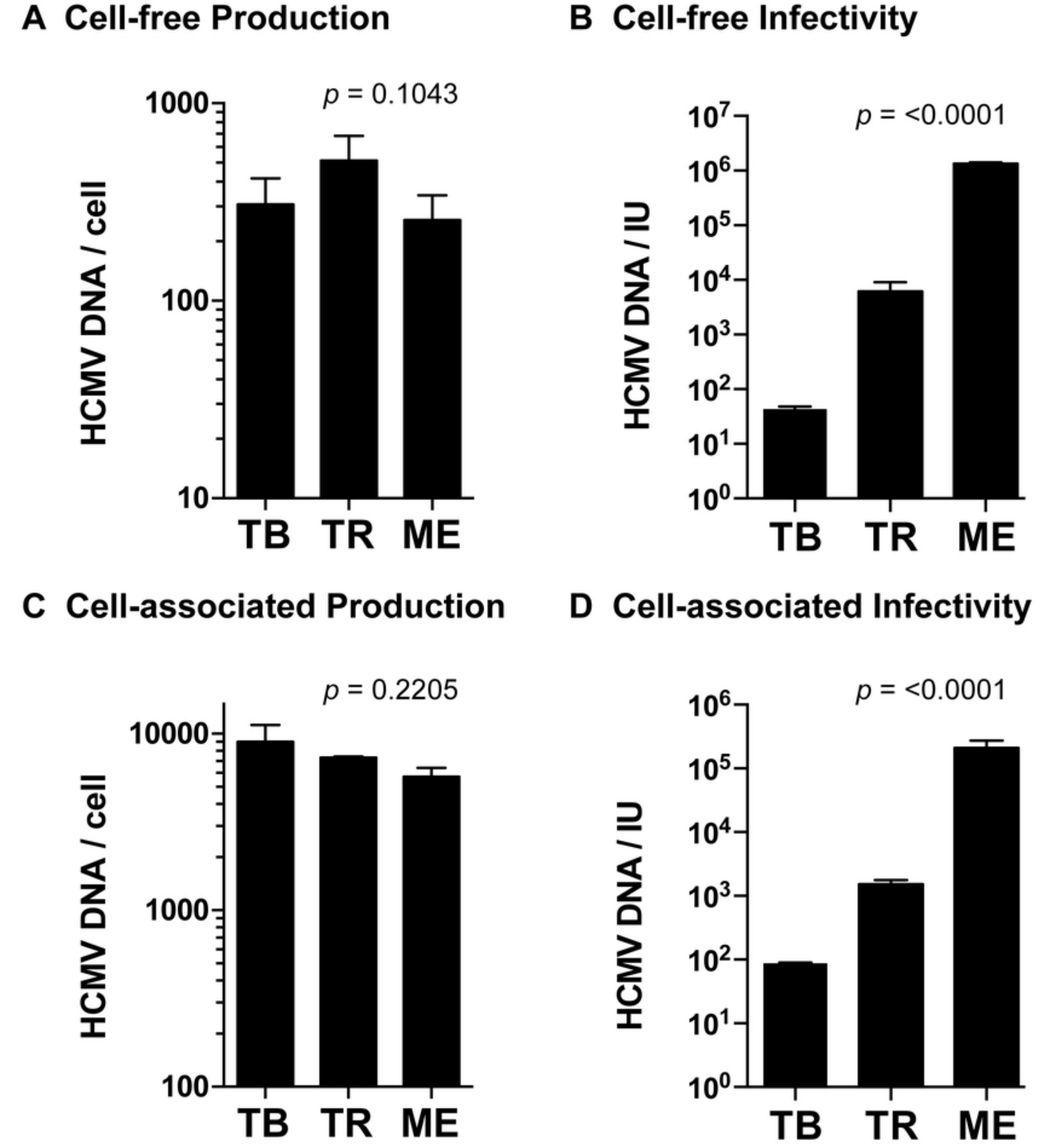
A Cell-free Production
p = 0.1043
HCMV DNA / cell
1000
100
10
TB
TR
ME
B Cell-free Infectivity
p = <0.0001
HCMV DNA / IU
10^7
10^6
10^5
10^4
10^3
10^2
10^1
10^0
TB
TR
ME
C Cell-associated Production
p = 0.2205
HCMV DNA / cell
10000
1000
100
TB
TR
ME
D Cell-associated Infectivity
p = <0.0001
HCMV DNA / IU
10^6
10^5
10^4
10^3
10^2
10^1
10^0
TB
TR
ME

Figure 3

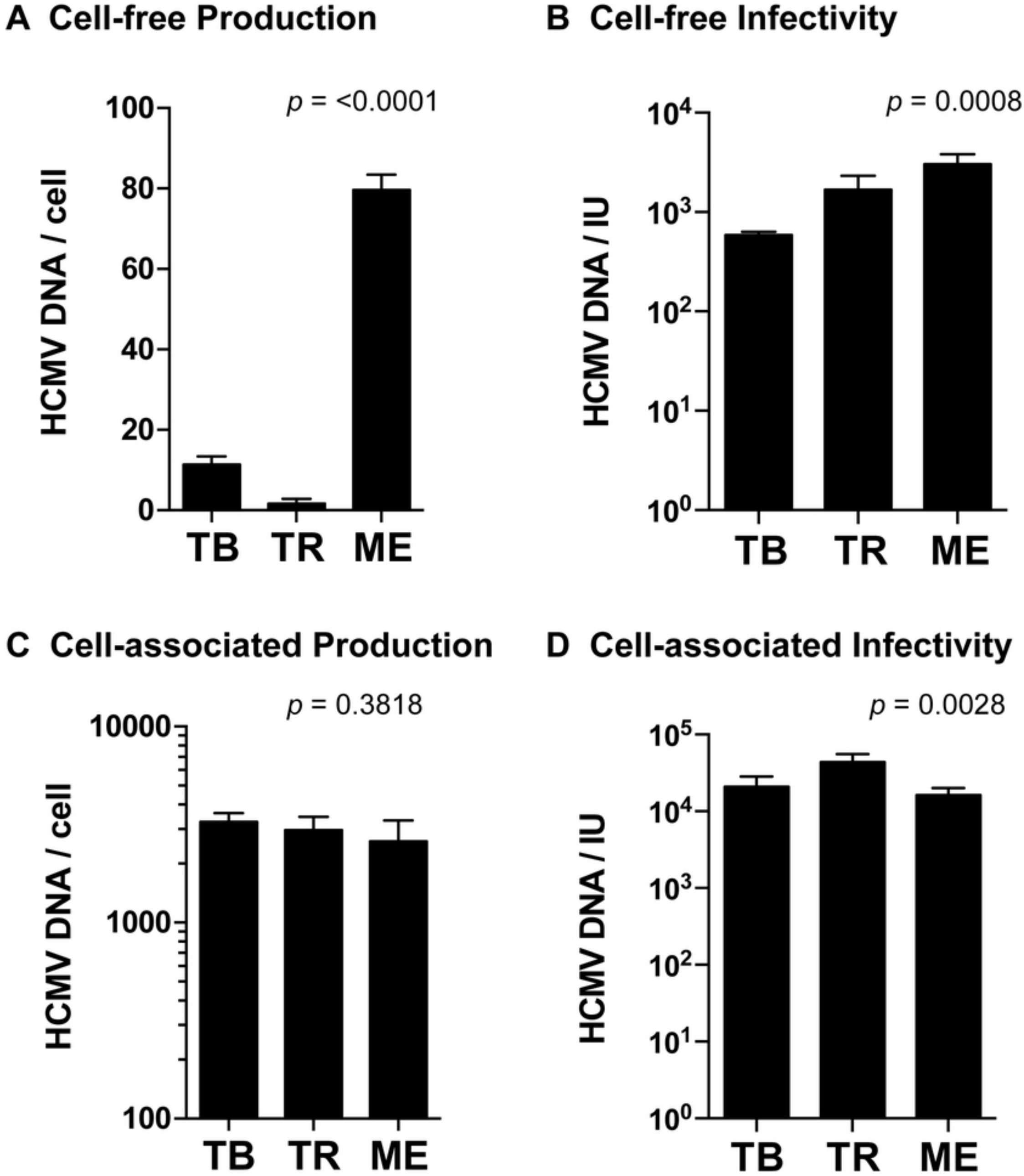
A Cell-free Production
p = <0.0001
HCMV DNA / cell
100
80
60
40
20
0
TB
TR
ME
B Cell-free Infectivity
p = 0.0008
HCMV DNA / IU
10^4
10^3
10^2
10^1
10^0
TB
TR
ME
C Cell-associated Production
p = 0.3818
HCMV DNA / cell
10000
1000
100
TB
TR
ME
D Cell-associated Infectivity
p = 0.0028
HCMV DNA / IU
10^5
10^4
10^3
10^2
10^1
10^0
TB
TR
ME

Figure 4

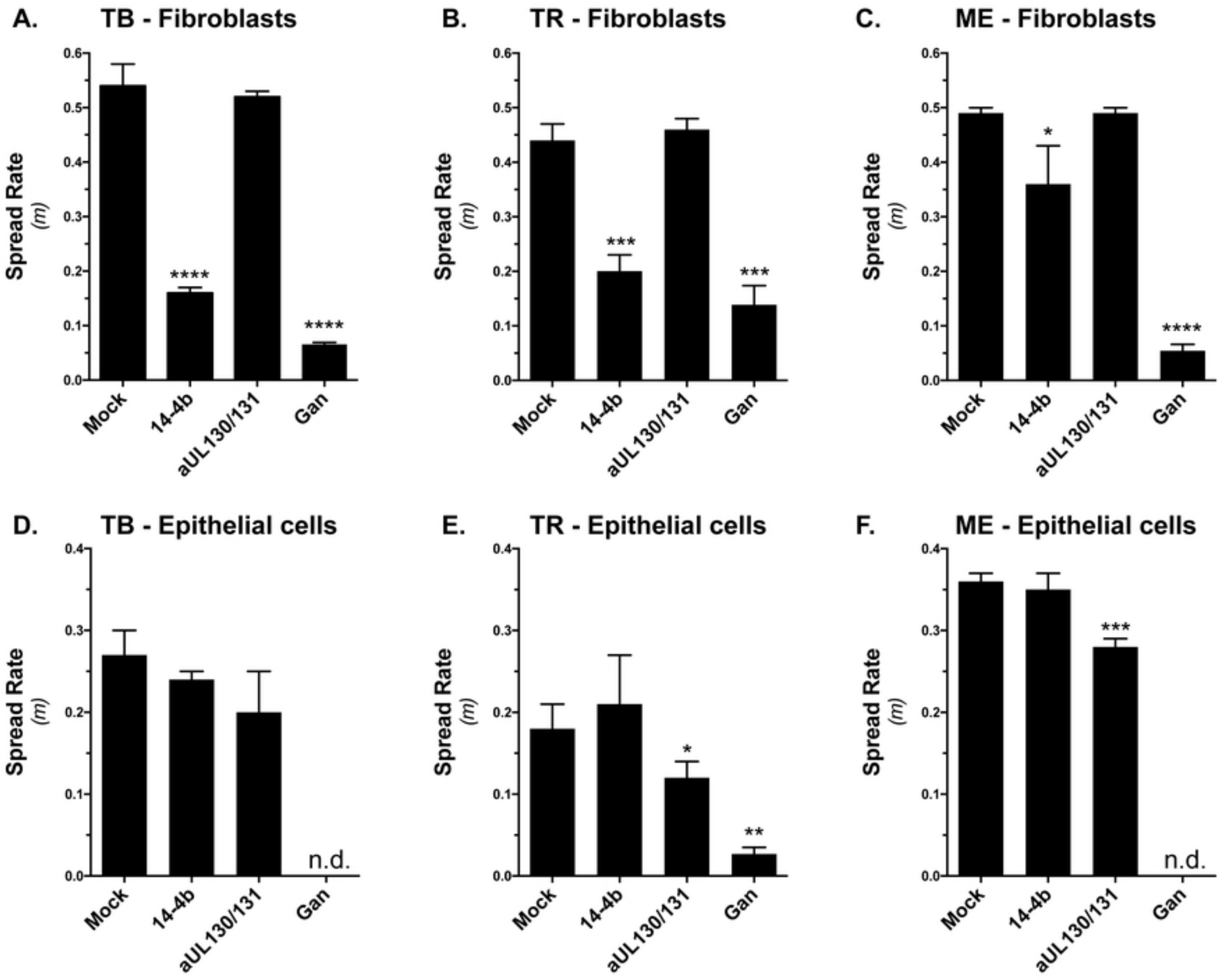
A.
TB - Fibroblasts
B.
TR - Fibroblasts
C.
ME - Fibroblasts
D.
TB - Epithelial cells
E.
TR - Epithelial cells
F.
ME - Epithelial cells
Spread Rate
(m)
Mock
14-4b
aUL130/131
Gan
****
***
**
*
n.d.

Figure 5

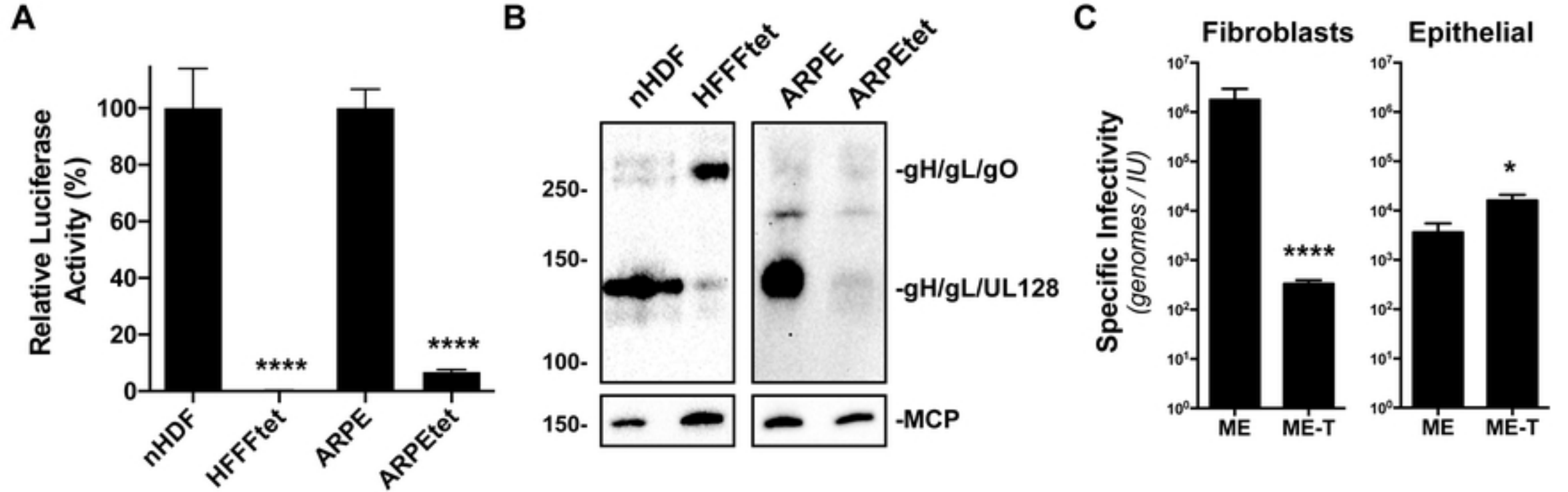
A
Relative Luciferase Activity (%)
100
80
60
40
20
0
****
****
nHDF
HFFFtet
ARPE
ARPEtet
B
nHDF
HFFFtet
ARPE
ARPEtet
250-
150-
100-
150-
-gH/gL/gO
-gH/gL/UL128
-MCP
C
Fibroblasts
Epithelial
Specific Infectivity
(genomes / IU)
****
*
ME
ME-T
ME
ME-T

Figure 6

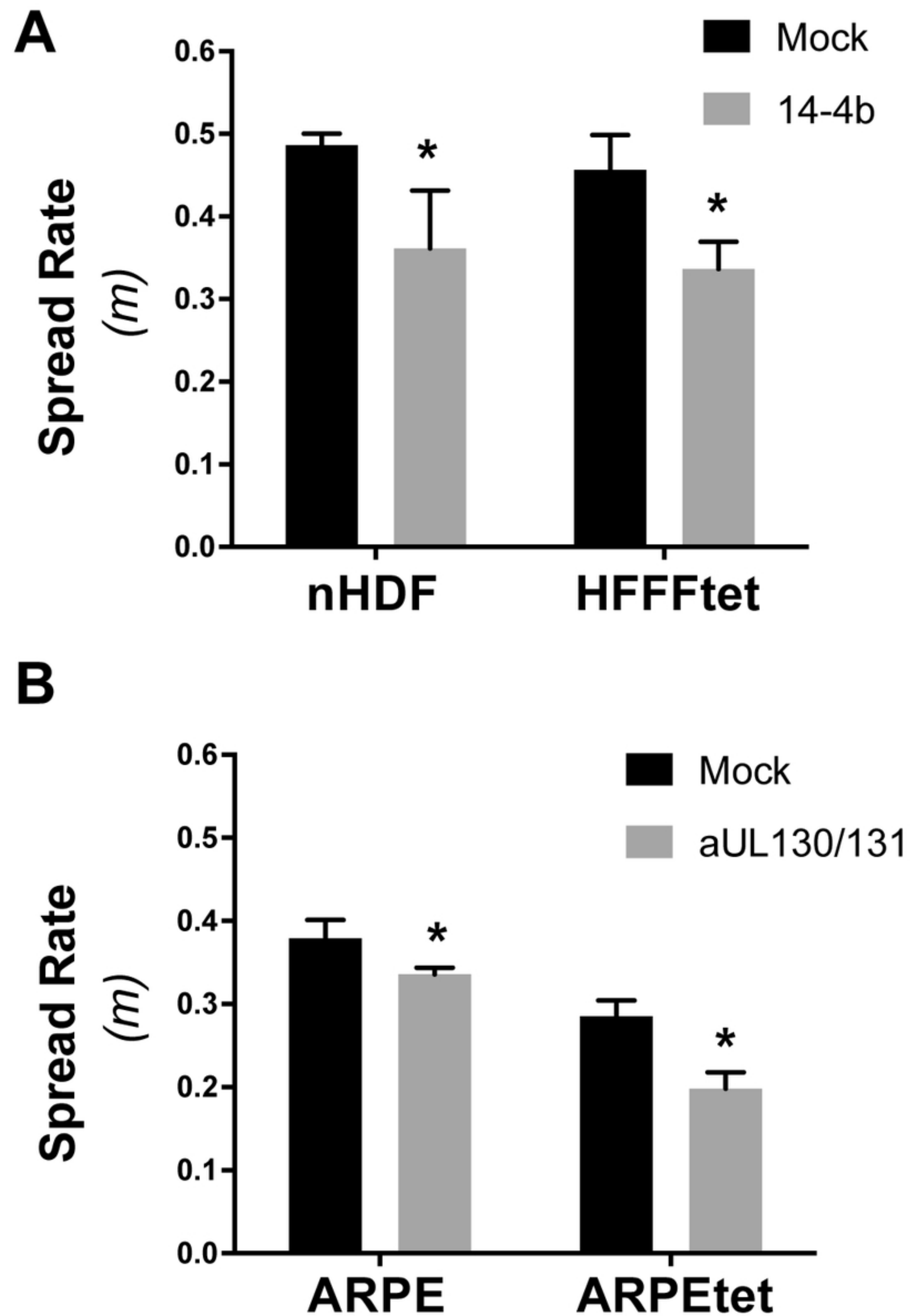
A
Mock
14-4b
Spread Rate
(m)
0.6
0.5
0.4
0.3
0.2
0.1
0.0
*
*
nHDF
HFFFtet
B
Mock
aUL130/131
Spread Rate
(m)
0.6
0.5
0.4
0.3
0.2
0.1
0.0
*
*
ARPE
ARPEtet

Figure 7

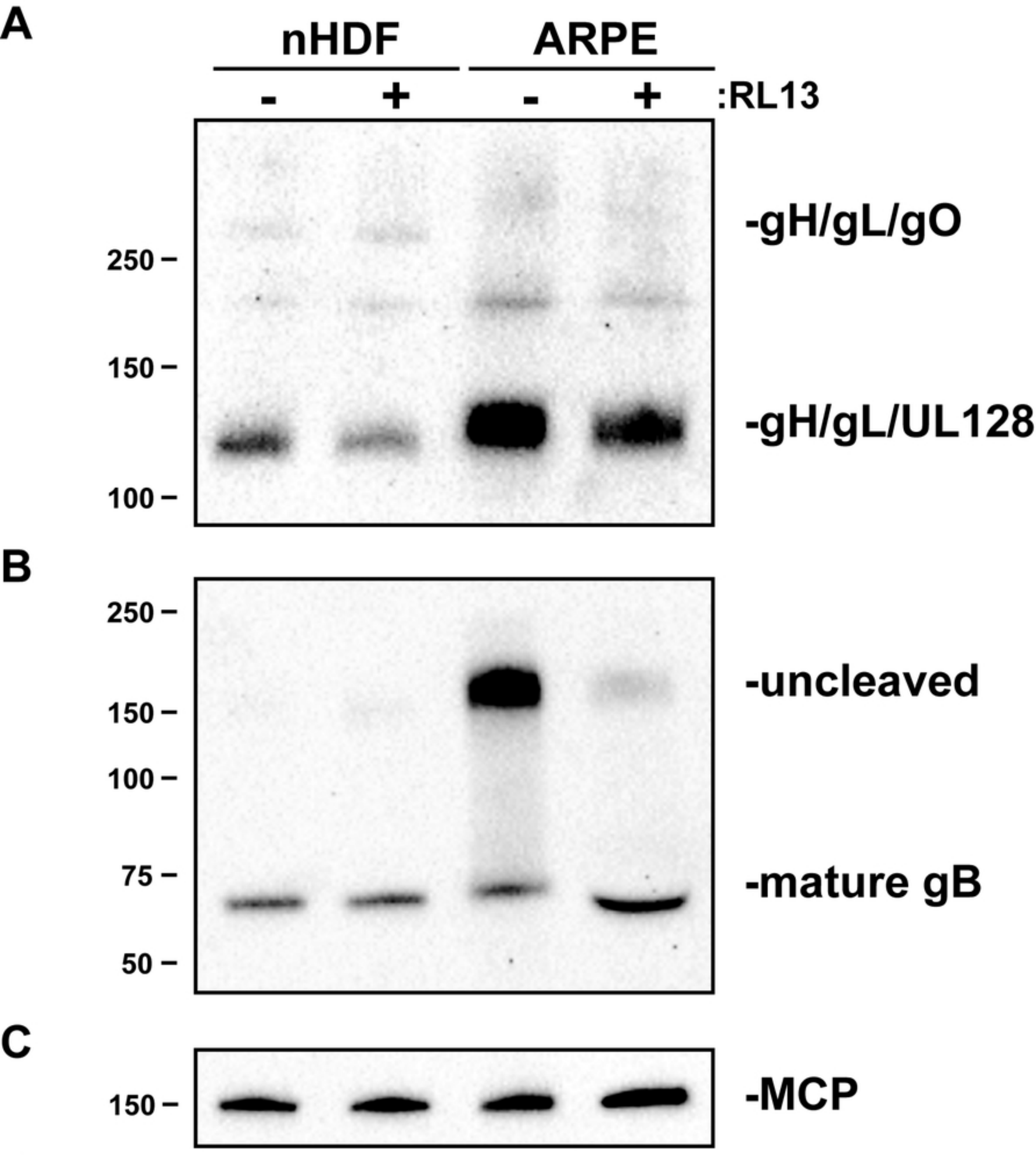
A
nHDF
ARPE
-
+
-
+
:RL13
250 –
150 –
100 –
-gH/gL/gO
-gH/gL/UL128
B
250 –
150 –
100 –
75 –
50 –
-uncleaved
-mature gB
C
150 –
-MCP

Figure 9

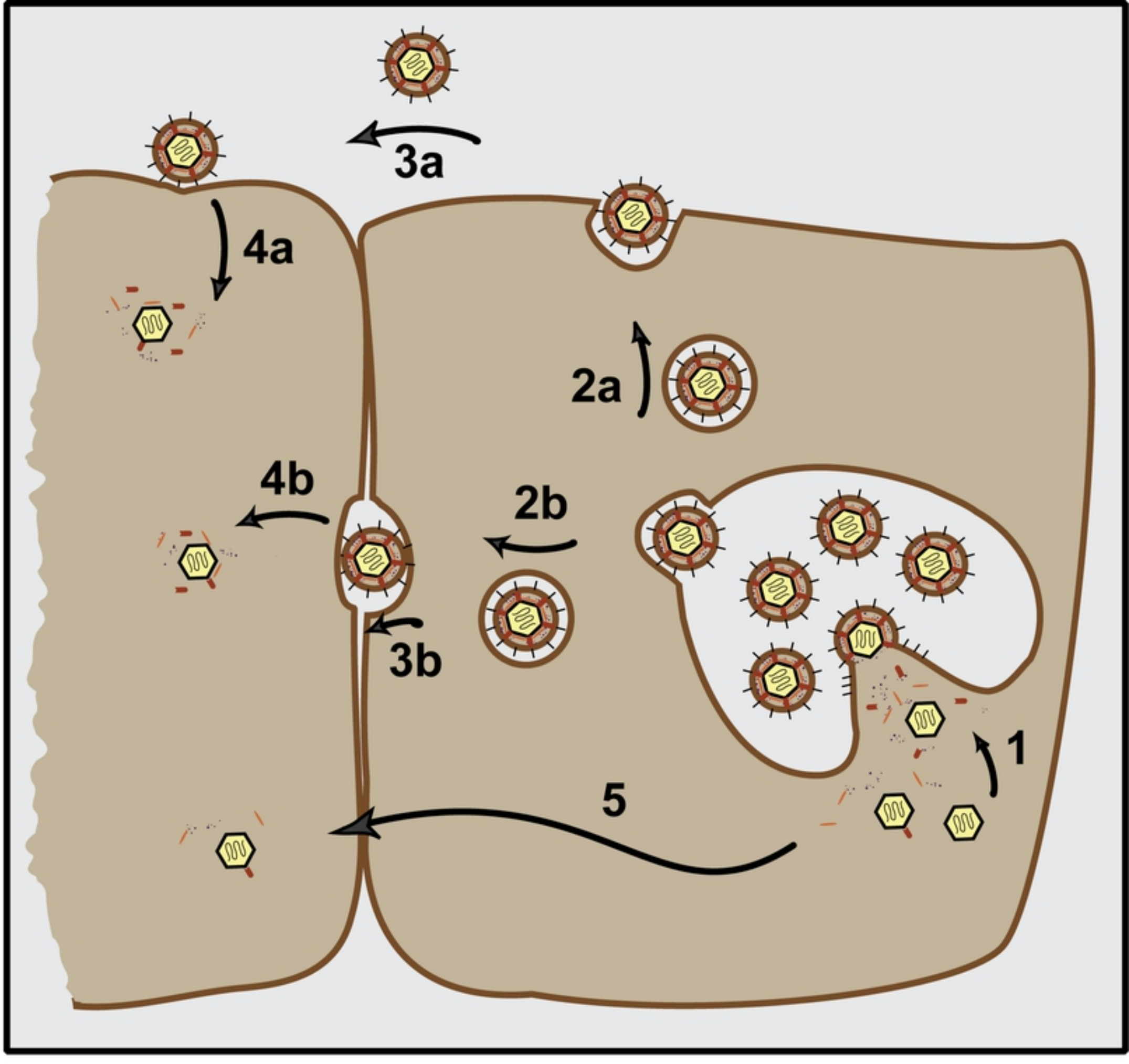

Figure 10